

Oxygen Isotope Analysis in a Land of Environmental Extremes: The Complexities of Isotopic Work in the Andes

K. J. KNUDSON*

Center for Bioarchaeological Research, School of Human Evolution and Social Change, PO Box 872402, Arizona State University, Tempe AZ 85287-2402, USA

ABSTRACT The Andes, which have a wide variety of diverse and distinct environmental zones ranging from the hyperarid coast to the high-altitude *altiplano*, are an ideal region in which to explore the use of oxygen isotope analyses to elucidate archaeological residential mobility. However, some questions remain, including the mobility of water through the environment, the seasonal and annual variability of precipitation in the past, and the role of water storage and beverage preparation techniques. Here, the advantages and disadvantages of oxygen isotope analysis in the Andes, and beyond, will be explored using oxygen isotope data from archaeological human enamel and bone from Peru, Bolivia and Chile (c. AD 1–1500). Although strontium isotope values from this region vary according to regional geology, oxygen isotope data do not always follow expected patterns based on known environmental variables, and probably reflect the movement of water throughout the Andes, complicating its use as a tool to identify human migration in the past. Copyright © 2009 John Wiley & Sons, Ltd.

Key words: biogeochemistry; migration; palaeodiet; Peru; Bolivia; Chile

Introduction

In the Andes, the wide variety of environmental zones, from the hyperarid coast to the high-altitude *altiplano*, has enabled an increasing number of scholars to use oxygen isotope analysis of archaeological human remains to investigate residential mobility. However, some questions remain. Because of the extreme environmental variability as well as the long history of bioarchaeological research and the growing numbers of heavy and light isotope analyses from the region, the Andes are an ideal area in

which to explore the complexities of using oxygen isotope analysis to identify archaeological residential mobility.

Here, the advantages and disadvantages of oxygen isotope analysis in the Andes, and beyond, will be explored using oxygen isotope data from archaeological human enamel and bone from Peru, Bolivia and Chile (c. AD 1–1500) (Figure 1). First, I briefly discuss oxygen isotope analysis and its use in identifying archaeological residential mobility. I then introduce the different environmental zones in the Andes, including temperature and precipitation regimes and expected and observed oxygen isotope signatures in meteoric water from each region. I then present oxygen isotope data from enamel and bone hydroxyapatite carbonate from individuals buried at a variety of different archaeological sites in

* Correspondence to: Center for Bioarchaeological Research, School of Human Evolution and Social Change, PO Box 872402, Arizona State University, Tempe, Arizona 85287-2402, United States. e-mail: kelly.knudson@asu.edu



Figure 1. Map of the Andes with the regions included in this study.

central and southern Peru, Bolivia and northern Chile. I conclude with a discussion of these data and their implications for oxygen isotope analyses.

Oxygen isotope analysis and archaeological residential mobility

In archaeology, the fact that oxygen isotope signatures vary according to a number of different environmental factors is used to identify residential mobility in the past. The ratio of ^{18}O and ^{16}O varies throughout the environment since water molecules that contain the lighter isotope of oxygen, ^{16}O , will evaporate more readily than water molecules that contain ^{18}O . On the other hand, the heavier isotope of oxygen will condense and fall out in precipitation more readily than ^{16}O . Rather than using ratios, oxygen isotope data is expressed using standard $\delta^{18}\text{O}$ notation, where $\delta^{18}\text{O} = \left(\frac{^{18}\text{O}/^{16}\text{O}_{\text{sample}}}{^{18}\text{O}/^{16}\text{O}_{\text{standard}}} - 1 \right) \times 1000$ (Craig, 1961b; Coplen, 1994). Therefore, $\delta^{18}\text{O}$ in precipitation, or meteoric water ($\delta^{18}\text{O}_{\text{mw}}$), decreases with

increasing altitude, increasing distance from the coast, increasing latitude, and decreasing temperature (Epstein & Mayeda, 1953; Craig, 1961a; Dansgaard, 1964; Gat, 1996; Koch, 1998; Bowen & Wilkinson, 2002).

Oxygen from drinking water and food sources is incorporated into phosphate and carbonate in hydroxyapatite in tooth enamel and bone, since $\delta^{18}\text{O}$ in body water equilibrates with $\delta^{18}\text{O}$ in hydroxyapatite at constant body temperature (Longinelli, 1984; Luz *et al.*, 1984; Luz & Kolodny, 1985). Scholars from a variety of disciplines have utilised $\delta^{18}\text{O}$ in various species to reconstruct palaeoclimate (e.g. Bryant *et al.*, 1994; Reinhard *et al.*, 1996; Stuart-Williams & Schwarcz, 1997; Shahack-Gross *et al.*, 2003; Zazzo *et al.*, 2006), animal migration and herding patterns (Killingley, 1980; Killingley & Lutcavage, 1983; Balasse *et al.*, 2006) and the provenance of plants and animals (Kelly *et al.*, 2005; Williams *et al.*, 2005a; Benson *et al.*, 2006; Dufour *et al.*, 2007). Archaeologists and bioarchaeologists have used differences in oxygen isotope signatures in archaeological human tooth enamel and bone to examine residential mobility when drinking water is presumably from local sources that reflect place of residence (e.g. White *et al.*, 1998, 2000, 2001, 2002, 2004b, 2004c, 2007; Prowse *et al.*, 2007), while contemporary human populations have been studied using hair and urine samples (O'Brien & Wooller, 2007; Ehleringer *et al.*, 2008).

Despite the promise of oxygen isotope analysis to elucidate archaeological residential mobility, questions remain. As with all isotopic techniques that use archaeological enamel and bone, biogenic signatures must be demonstrated. Numerous studies have demonstrated that enamel oxygen phosphate ($\delta^{18}\text{O}_{\text{p}}$), and oxygen carbonate ($\delta^{18}\text{O}_{\text{c}}$) to a lesser extent, is resistant to diagenetic contamination, and there are a number of methods to identify contamination if it exists (Lee-Thorp & Merwe, 1991; Sharp *et al.*, 2000; Lee-Thorp, 2002; Lee-Thorp & Sponheimer, 2003; Shahack-Gross *et al.*, 2003; Zazzo *et al.*, 2004). Bone, particularly fossilised specimens, is more susceptible to diagenetic contamination (Nelson *et al.*, 1986; Iacumin *et al.*, 1996b; Sharp *et al.*, 2000; Hedges, 2002; Lee-Thorp, 2002; Lee-Thorp & Sponheimer, 2003; Shahack-Gross *et al.*, 2003). In addition to post-depositional

contamination, other factors that can affect oxygen isotope signatures include heating above 300°C (Munro *et al.*, 2007).

If biogenic oxygen isotope signatures are retained, determining the relationship between observed $\delta^{18}\text{O}_{\text{mw}}$ and the water sources in the diet is imperative. While some of the oxygen in archaeological human remains comes from the atmosphere via inhalation and some oxygen comes from food consumed, most oxygen comes from imbibed water (Longinelli, 1984; Luz *et al.*, 1984; Luz & Kolodny, 1985). This water may derive from a number of sources, such as rainwater collected in cisterns, river water, snow or glacial meltwater, or groundwater obtained through wells. Storage and preparation of water or other oxygen sources will also affect oxygen isotope signatures. For example, oxygen in beverages that have been boiled, like Andean *chicha*, or maize beer, will be enriched in ^{18}O , since ^{16}O will evaporate during boiling (Wilson *et al.*, 2007; see also Wright & Schwarcz, 1998). All of these factors must be taken into account rather than relying on observed $\delta^{18}\text{O}_{\text{mw}}$ values in precipitation; these factors will be discussed below for the study region.

When using enamel oxygen isotope signatures, the effect of oxygen in breast milk should also be taken into account. As discussed above, enamel samples are preferred because of their relative lack of diagenetic contamination. However, children who are breastfeeding will exhibit enamel oxygen isotope signatures that are enriched in ^{18}O (Roberts *et al.*, 1988). This is because the oxygen in body water, and hence breast milk, is enriched in ^{18}O relative to imbibed water since expired water contains more ^{16}O (Roberts *et al.*, 1988). While this enrichment is very useful when examining the weaning process in prehistory (Wright & Schwarcz, 1999; White *et al.*, 2004a; Williams *et al.*, 2005b; Dupras & Tocheri, 2007), it could also complicate interpretations of residential mobility that rely on oxygen isotope signatures in enamel that may have formed while an individual was consuming breast milk. It is possible, however, to use $\delta^{13}\text{C}$ in hydroxyapatite carbonate to examine the introduction of other foods during the weaning process (Wright & Schwarcz, 1999; White *et al.*, 2004a; Williams *et al.*, 2005b; Dupras &

Tocheri, 2007), and to examine similar shifts using carbon and nitrogen isotope data from bone collagen (Herring *et al.*, 1998; Schurr, 1998; Wright & Schwarcz, 1999; Dupras *et al.*, 2001; Richards *et al.*, 2002; Fuller *et al.*, 2003, 2006; Williams *et al.*, 2005b; Dupras & Tocheri, 2007; Turner *et al.*, 2007) and strontium and calcium concentrations (Mays, 2003). Understanding the prehistoric weaning process and its effects on oxygen isotope signatures in enamel or in the bone of subadults is an integral aspect of residential mobility studies that use oxygen isotopes.

Previous work on Andean residential mobility

Much of the previous work on Andean residential mobility has utilised strontium isotope analysis to elucidate migration during the Early Intermediate Period (c. AD 1–600) Nasca polity (Buzon *et al.*, 2008; Knudson *et al.*, in press), Middle Horizon (c. AD 600–1100) Tiwanaku and Wari polities (Knudson, 2004, 2007, 2008; Knudson *et al.*, 2004, 2005; Tung & Knudson, 2006, 2008; Knudson & Price, 2007; Knudson & Tung, 2007; Knudson & Blom, in press), the Late Intermediate Period (c. AD 1100–1400) Chiribaya polity (Knudson, 2004; Knudson & Buikstra, 2007; Knudson & Price, 2007), and the Late Horizon Inka empire (c. AD 1400–1532) (Turner *et al.*, 2006, 2008; Andrushko *et al.*, 2007, in press; Wilson *et al.*, 2007). Fewer research projects have used oxygen isotope analysis to look at Andean mobility, although scholars are beginning to combine strontium and oxygen isotopes to look at mobility across different geological and environmental zones (Tomczak, 2001; Turner *et al.*, 2006, 2008; Knudson & Price, 2007; Slovak, 2007). However, the environmental extremes in the Andes would seem to be an ideal region in which to apply oxygen isotope analysis, as I will discuss below.

Oxygen isotope signatures in the Andes

Here, I review the major environmental zones of the Andes, following the Quechua nomenclature

provided by Javier Pulgar Vidal (1981); while eight zones are defined, I focus on the five zones with the highest populations in the western Andes, rather than discussing the eastern slopes of the Andes and the Amazon. I also discuss the expected and observed oxygen isotope signatures for each zone. Finally, I finish with a discussion of El Niño and its role in Andean environmental variability.

The coastal chala zone

The coast, or *chala*, of Peru and northern Chile is located below 500 metres above sea level (m.a.s.l.) and is extremely arid, with many areas receiving less than 50 mm of precipitation each year (Pulgar Vidal, 1981; Tapley & Waylen, 1990). In fact, the Atacama Desert of southern Peru and northern Chile is one of the driest deserts in the world, and receives 0–20 mm of precipitation each year (e.g. Núñez *et al.*, 2002; Houston & Hartley, 2003; Houston, 2006). Much of the precipitation in the *chala* zone comes from heavy fog, called *garúa*, between June and November. However, the many rivers that originate in the Andes and run west to the coast ensure that the coastal valleys are habitable and cultivable. With temperatures that can reach 25–35°C during the day, irrigation agriculture in the coastal valleys produces beans (*Phaseolus vulgaris*), squashes (*Cucurbita* sp.), maize (*Zea mays*), peanuts (*Arachis hypogaea*), and fruits like cherimoya (*Annona chirimola*) and lúcuma (*Pouteria lucuma*). Cotton (*Gossypium barbadense*) was an important crop, and sugar cane (*Saccharum* sp.) became cultivated widely in the 20th century. In addition to agricultural products, the marine ecosystem is very rich in small fish like anchovies (*Engraulis* sp.) and larger fish like tuna (*Thunnus* sp.). Finally, the coastal plant communities called *lomas*, which contain epiphytic plants adapted to the fog, have resources for both humans and camelids (Masuda, 1985).

Given the low altitude and short distance to the ocean, expected oxygen isotope signatures ($\delta^{18}\text{O}_{\text{mw}}$) in the *chala* precipitation should be relatively high. For example, between 1988 and 2002, observed $\delta^{18}\text{O}_{\text{mw(V-SMOW)}} = -5.6\text{‰} \pm 2.3\text{‰}$ ($n = 16$, 1σ) in La Serena, Chile, which

is located on the Pacific Ocean 470 km north of Santiago, Chile (IAEA/WMO, 2006; see also Squeo *et al.*, 2006). Fog from the *lomas* will probably be enriched and exhibit higher $\delta^{18}\text{O}_{\text{mw}}$ than the rainwater along the coast (Aravena *et al.*, 1989; Ingraham & Matthews, 1995; Scholl *et al.*, 2002; Squeo *et al.*, 2006). In addition, the water in the arid soils along the coast will be enriched in ^{18}O relative to the precipitation that falls because of evaporation (Gat, 1996). However, the water imbibed by individuals living on the coast will not consist solely of coastal precipitation, given the extreme aridity. Much of the usable water in the *chala* consists of rainwater, snowmelt and glacial ice melt from higher altitudes that flows down in rivers. Precipitation from higher altitudes is also incorporated into underground aquifer systems that are accessed through wells and springs (Magaritz *et al.*, 1990; Squeo *et al.*, 2006). River water in the *chala* should therefore contain water with lower $\delta^{18}\text{O}$ from higher-altitude precipitation. In addition, evaporation that occurs while the water flows to the Pacific Ocean ensures that the river waters will be enriched in ^{18}O , which will result in a higher $\delta^{18}\text{O}$ signature. Surface water from coastal rivers in northern Peru exhibits $\delta^{18}\text{O}_{\text{(V-SMOW)}} = -3.3\text{‰}$ to -5.7‰ , while groundwater from springs in the region exhibits $\delta^{18}\text{O}_{\text{(V-SMOW)}} = -4.2\text{‰}$ to -5.1‰ (IAEA/WMO, 2006).

The mid-altitude yungas

The mid-altitude *yungas* zones, located between 500–2300 m.a.s.l., are characterised by more precipitation and milder temperatures than the coastal regions (Pulgar Vidal, 1981). Between December and May, 50–200 mm of precipitation from the prevailing winds that blow from the southwest falls in the *yungas* zone (Tapley & Waylen, 1990). Conditions are ideal for a number of agricultural crops, such as maize (*Zea mays*), coca (*Erythroxylum coca*), ají peppers (*Capsicum* sp.), and fruits like guayaba (*Psidium guajava*), cherimoya (*Annona chirimola*) and lúcuma (*Pouteria lucuma*) (e.g. Brush, 1982).

Since the altitude in the *yungas* is slightly higher than the *chala* zone, expected oxygen isotope signatures ($\delta^{18}\text{O}_{\text{mw}}$) in the *yungas*

precipitation should be lower. While the Global Network of Isotopes in Precipitation does not currently include *yungas* precipitation values (IAEA/WMO, 2006), these altitudinal effects are apparent in observed $\delta^{18}\text{O}$ from springs located at different altitudes but at approximately the same latitude and longitude, where $\delta^{18}\text{O}_{(\text{V-SMOW})} = -8.6\text{‰}$ (2020 m.a.s.l.), $\delta^{18}\text{O}_{(\text{V-SMOW})} = -7.1\text{‰}$ (1450 m.a.s.l.), $\delta^{18}\text{O}_{(\text{V-SMOW})} = -6.1\text{‰}$ (990 m.a.s.l.), and $\delta^{18}\text{O}_{(\text{V-SMOW})} = -5.1\text{‰}$ (105 m.a.s.l.) (IAEA/WMO, 2006). In general, water sources in the *yungas* will consist of a mixture of precipitation, and rivers containing precipitation and glacier melt from higher altitudes; springs may also supply drinking water and irrigation water.

The high-altitude quechua and suni zones

The high-altitude *quechua* and *suni* zones are also agriculturally productive zones, although they are located at 2300–3500 m.a.s.l. and 3500–4000 m.a.s.l, respectively (Pulgar Vidal, 1981). Given the higher altitudes, temperatures are cooler with large diurnal ranges of 10°C (Pulgar Vidal, 1981). Here, extensive systems of agricultural terraces are used to grow high-altitude crops such as quinoa (*Chenopodium quinoa*), potatoes (*Solanum tuberosum*) and oca (*Oxalis tuberosa*), which are supplemented by camelids, guinea pigs and wild plants (e.g. Browman, 1981; Brush, 1982). While still semi-arid, precipitation in these zones is 500–1000 mm annually and is predominantly derived from the west (Tapley & Waylen, 1990).

Compared with the *yungas* and *chala* zones, $\delta^{18}\text{O}_{\text{mw}}$ should be lower in the higher-altitude *quechua* and *suni* zones. Given the higher rates of rainfall in the *quechua* and *suni* zones, oxygen in precipitation could have a larger effect on $\delta^{18}\text{O}$ in human food and water sources. However, river water that contains precipitation from higher altitudes as well as snow and glacial melt could also be an important source of oxygen in the *quechua* and *suni* zones. Fractionation effects mean that snowmelt and glacial melt will be depleted when compared with the oxygen isotope signatures of the snowpack itself (Stichler & Schotterer, 2000).

The high mountains and plains of the puna

The *puna* is located between 4000–4800 m.a.s.l. and consists of grasslands and alpine tundra (Pulgar Vidal, 1981). In the northern Andes, where the highest altitude zones are lower in elevation and generally wetter, this area is called the *páramo*; in the southern Andes, the *altiplano*, or high plain, runs between the two mountain ranges of the Andes. While median annual temperatures only vary by 5°C , temperatures can vary as much as 20°C in a 24-hour period (Pulgar Vidal, 1981; Brush, 1982; Binford & Kolata, 1996). *Puna* precipitation takes the form of rain, hail and snow, and averages 200–1500 mm per year, with the driest areas in the south (Tapley & Waylen, 1990; Roche *et al.*, 1991; Vuille & Ammann, 1997; Núñez *et al.*, 2002). The precipitation at these altitudes is derived from both the Amazonian and Pacific air masses (Grootes & Stuiver, 1989; Binford & Kolata, 1996). However, most moisture comes from the east, and east-facing slopes have more precipitation than those facing west (Binford & Kolata, 1996). The *puna* is an ideal environment for camelids, and llamas (*Lama glama*) and alpacas (*Lama pacos*) are herded in the area while wild camelids, including guanacos (*Lama guanicoe*) and vicuñas (*Lama vicugna*), are also found at these altitudes.

In the Andean *puna* and *altiplano*, observed oxygen isotope signatures in precipitation in La Paz, Bolivia, were $\delta^{18}\text{O}_{\text{mw(V-SMOW)}} = -13.3\text{‰}$ to -10.8‰ between 1996–2001, while precipitation near Puno, Peru, exhibited $\delta^{18}\text{O}_{\text{mw(V-SMOW)}} = -13.3\text{‰} \pm 5.3\text{‰}$ ($n = 20$, 1σ) between 2001–2002 (IAEA/WMO, 2006). Similarly, precipitation measured on Isla Taquile, Lake Titicaca, Peru, exhibited $\delta^{18}\text{O}_{\text{mw(V-SMOW)}} = -17.6\text{‰} \pm 4.5\text{‰}$ ($n = 17$, 1σ) between 2001–2002 (IAEA/WMO, 2006). While precipitation will contribute to the oxygen isotope signatures in water sources in the *puna*, rainwater, snowmelt and glacial melt will also contribute (Gat, 1996). At high altitudes, $\delta^{18}\text{O}_{\text{mw}}$ in precipitation reflects both its origin in the Atlantic and, in the case of snow and glaciers, complex processes of deposition and modification after deposition (Grootes & Stuiver, 1989). For example, surface snow on the Quelccaya ice cap increased from $\delta^{18}\text{O}_{\text{mw(V-SMOW)}} = -10.4\text{‰}$ to $\delta^{18}\text{O}_{\text{mw(V-SMOW)}} = -4.1\text{‰}$

over a 12-day period because of freezing, thawing and evaporation (Grootes & Stuiver, 1989). Groundwater oxygen isotope signatures are less variable than precipitation values, and reflect the contributions of precipitation, glacial melt and evaporation. For example, observed oxygen isotope signatures in Lake Titicaca Basin surface water were $\delta^{18}\text{O}_{\text{mw(V-SMOW)}} = -17.6\text{‰}$ to -12.6‰ , while the Llinqui River exhibited $\delta^{18}\text{O}_{\text{mw(V-SMOW)}} = -12.4\text{‰} \pm 2.2\text{‰}$ ($n = 7$, 1σ) in 1998–2001 (IAEA/WMO, 2006). A spring near Juli, Peru, exhibited $\delta^{18}\text{O}_{\text{mw(V-SMOW)}} = -16.7\text{‰} \pm 0.3\text{‰}$ ($n = 7$, 1σ) in 1998–1999, which probably reflects evaporation effects as well as mixing from various sources (IAEA/WMO, 2006).

El Niño and its role in Andean environmental variability

A major source of Andean environmental variability during the Holocene is caused by El Niño–Southern Oscillation (ENSO) events (Thompson *et al.*, 1984; Rollins *et al.*, 1986; Sandweiss *et al.*, 1996, 2001; Magiligan & Goldstein, 2001; Dillehay & Kolata, 2004; Carré *et al.*, 2005). At irregular intervals between every 25–50 years, the union of an eastern equatorial ocean current with a warmer countercurrent off the coast of Ecuador dramatically increases the ocean temperature. As ocean temperatures rise, marine animals either die or migrate to cooler waters. In addition to major disruptions in the marine ecosystem, ENSO events cause torrential rainfall on the coast, where areas that generally receive very little rainfall are inundated with 1000–4000 mm of rainfall over a short period and often suffer floods and landslides (Caviedes, 1975; Waylen & Caviedes, 1986; Tapley & Waylen, 1990). In contrast, the high-altitude regions receive less precipitation and endure droughts (Caviedes, 1984; Tapley & Waylen, 1990). In the past and today, highland farmers rely on the poor visibility of the stars in the Pleiades in June to predict upcoming ENSO droughts and irrigate their crops accordingly (Orlove *et al.*, 2000).

There are a variety of different lines of evidence that can be used to identify ENSO events in the past. For example, some scholars have identified ENSO events based on oxygen

isotope analysis of sea shells (Carré *et al.*, 2005, 2006) or fish otoliths (Andrus *et al.*, 2002, 2003; see also Bearez *et al.*, 2003), while others have identified major flood events on the coast (Moore, 1991; Satterlee, 1993; Reycraft, 2000; Magiligan & Goldstein, 2001; Van Buren, 2001; Zaro & Umire Alvarez, 2005). Years in which ENSO events occurred in the past should be characterised by a higher input of coastal precipitation into the water sources imbibed by coastal inhabitants (e.g. Squeo *et al.*, 2006).

Past and present climate in the Andes: the use of contemporary data to interpret archaeological isotope signatures

In general, the basic Andean environmental patterns described above have not changed for the last 2000 years (Shimada *et al.*, 1991; Baied & Wheeler, 1993; Messerli *et al.*, 1993; Bobst *et al.*, 2001; Hartley & Chong, 2002; Núñez *et al.*, 2002; Bush *et al.*, 2005; Ramirez *et al.*, 2007). However, an understanding of the environmental conditions at particular sites and during particular time periods is of utmost importance when using oxygen isotope signatures to reconstruct residential mobility. For example, palaeoclimate in the *altiplano*, the Lake Titicaca Basin, which consists of both *suní* and *puna* zones, and the San Pedro de Atacama region of northern Chile was not significantly different from the current climate (Messerli *et al.*, 1993; Bobst *et al.*, 2001; Núñez *et al.*, 2002). However, there is evidence for a drought in the Lake Titicaca Basin and *altiplano* between approximately AD 1100–1300 (Thompson *et al.*, 1979, 1985, 1998; Ortloff & Kolata, 1993; Binford *et al.*, 1997). While modern precipitation values are useful in examining general trends in oxygen isotope variability, understanding the oxygen isotope signatures in the water sources consumed and the climate for the time periods and regions under investigation is vital. Here, I present oxygen isotope signatures from enamel and bone hydroxyapatite carbonate from different regions in the Andes. By comparing these data with strontium isotope data from these individuals, which helps determine geographical origins based largely on regional

geology (Bentley, 2006), the variability of oxygen isotope signatures in the Andes can be explored.

Laboratory methodology for isotope analyses

Sampling strategy

Samples included in this study were collected from archaeological sites in the following regions: Nazca Drainage (southern Peru), Moquegua Valley (far southern Peru), Lake Titicaca Basin (western Bolivia), and the San Pedro de Atacama oases (northern Chile) (Table 1, Figure 1). These samples therefore cover a variety of environmental zones, from the *chala* to the *puna*. The enamel and bone samples were collected to reflect a minimum 10–15% representative sample from each site. Finally, all samples were included in previous and ongoing residential mobility studies that utilised strontium isotopes (Knudson *et al.*, 2004; Knudson, 2007, 2008; Knudson & Price, 2007; Knudson & Blom, in press), so that each sample has both strontium and oxygen isotope data for comparison.

Laboratory methodology for oxygen and carbon isotope analyses

Archaeological enamel and bone samples were prepared at the Laboratory for Archaeological Chemistry at the University of Wisconsin at Madison, and at the Archaeological Chemistry Laboratory at Arizona State University. Based on established methodologies, enamel or bone powder was treated with 2% NaOCl and 0.1 M CH₃COOH (Koch *et al.*, 1997). Preliminary oxygen isotope analysis was performed at the Stable Isotope Laboratory in the Department of Geosciences at the University of Arizona using a Finnigan MAT 253 mass spectrometer equipped with a Kiehl III automated carbonate sampling device, where replicates of NBS-19 resulted in a reproducibility of $\pm 0.1\%$ for $\delta^{18}\text{O}$. The majority of the samples were analysed in the W.M. Keck Laboratory for Environmental Biogeochemistry at Arizona State University on a Finnigan MAT 252 mass spectrometer. Replicates of NBS-19

resulted in a reproducibility of $\pm 0.15\%$ for $\delta^{18}\text{O}$ and $\pm 0.04\%$ for $\delta^{13}\text{C}$. Oxygen and carbon isotope ratios ($\delta^{18}\text{O}_c$, $\delta^{13}\text{C}_c$) are reported relative to the V-PDB (Vienna PeeDee belemnite) carbonate standard and are expressed in per mil (‰) using the following standard formula: $\delta^{18}\text{O} = (((^{18}\text{O}/^{16}\text{O}_{\text{sample}})/(^{18}\text{O}/^{16}\text{O}_{\text{standard}})) - 1) \times 1000$ (Craig, 1961b; Coplen, 1994). In order to compare the observed $\delta^{18}\text{O}_{c(\text{VPDB})}$ values with the observed $\delta^{18}\text{O}_{\text{mw}}$ (V-SMOW) values in the Andes, the conversion equations listed below were used:

$$\begin{aligned} \delta^{18}\text{O}_{\text{VSMOW}} &= (1.03091 \times (\delta^{18}\text{O}_{\text{VPDB}})) \\ &+ 30.91 \text{ (Coplen } et al., 1983) \\ \delta^{18}\text{O}_{\text{VPDB}} &= (0.97002 \times \delta^{18}\text{O}_{\text{VSMOW}}) - 29.98 \\ &\text{(Coplen } et al., 1983) \\ \delta^{18}\text{O}_{c(\text{VSMOW})} &= (8.5 + (\delta^{18}\text{O}_{p(\text{VSMOW})})) / \\ &0.98 \text{ (Iacumin } et al., 1996a) \\ \delta^{18}\text{O}_{p(\text{VSMOW})} &= (0.78 \times (\delta^{18}\text{O}_{\text{dw}(\text{VSMOW})})) \\ &+ 22.70 \text{ (Luz } et al., 1984) \\ \delta^{18}\text{O}_{p(\text{VSMOW})} &= (0.64 \times (\delta^{18}\text{O}_{\text{dw}(\text{VSMOW})})) \\ &+ 22.37 \text{ (Longinelli, 1984)} \end{aligned}$$

Laboratory methodology for strontium isotope analyses

Strontium isotope data provide an independent line of evidence for archaeological residential mobility in the Andes. Archaeological enamel and bone samples were prepared at the Laboratory for Archaeological Chemistry at the University of Wisconsin at Madison, and at the Archaeological Chemistry Laboratory at Arizona State University. Enamel and bone samples were mechanically cleaned by abrasion and bone samples were also chemically cleaned with a series of weak acetic acid washes and then ashed (see Sillen, 1989; Sillen & LeGros, 1991; Sillen & Sealy, 1995). Strontium isotope ratios were obtained at the Geochronology and Isotope Geochemistry Laboratory at the University of North Carolina at Chapel Hill, and at the W.M. Keck Foundation Laboratory for Environmental Biogeochemistry in the School of Earth and Space Exploration at Arizona State University. The strontium was separated from the sample matrix with EiChrom SrSpec resin based on published methodologies (Knudson, 2007;

Table 1. Isotope data from archaeological human remains from the Andes

Site, country	Laboratory number	Specimen number	Material ^a	⁸⁷ Sr/ ⁸⁶ Sr ^b	$\delta^{18}\text{O}_{\text{VPDB}}$ ^{c,d}	$\text{d}^{18}\text{O}_{\text{dw(V-SMOW)}}$
<i>San Pedro de Atacama</i>						
Casa Parroquial, Chile	ACL-0045	CAP-0001	LLP2	0.70781	-3.9	-6.2
Casa Parroquial, Chile	ACL-0046	CAP-0001	LRM1	0.70767	-3.4	-5.6
Casa Parroquial, Chile	ACL-0049	CAP-0001	R rib	0.70758	-6.0	-8.9
Casa Parroquial, Chile	ACL-0051	CAP-0002	LLM2	0.71456	-5.6	-8.4
Casa Parroquial, Chile	ACL-0052	CAP-0002	L rib	0.70757	-6.3	-9.4
Casa Parroquial, Chile	ACL-0056	CAP-0008	LRM2	0.70778	-4.7	-7.2
Casa Parroquial, Chile	ACL-0060	CAP-0010	ULM1	0.70785	-3.8	-6.1
Casa Parroquial, Chile	ACL-0061	CAP-0010	URM2	0.70798	-4.0	-6.4
Casa Parroquial, Chile	ACL-0062	CAP-0010	LRM3	0.70772	-4.8	-7.4
Casa Parroquial, Chile	ACL-0065	CAP-0011	LLM3	0.70786	-4.2	-6.6
Casa Parroquial, Chile	ACL-0066	CAP-0011	R rib	0.70779	-7.7	-11.2
Casa Parroquial, Chile	ACL-0067	CAP-0011	L femur	0.70757	-6.5	-9.6
Casa Parroquial, Chile	ACL-0071	CAP-0014	R femur	0.70775	-7.6	-11.0
Casa Parroquial, Chile	ACL-0076	CAP-0020	LRM3	0.70775	-4.0	-6.4
Casa Parroquial, Chile	ACL-0077	CAP-0020	R rib	0.70752	-7.4	-10.7
Casa Parroquial, Chile	ACL-0079	CAP-0022	Molar	0.70859	-5.2	-8.0
Casa Parroquial, Chile	ACL-0080	CAP-0022	Molar	0.70894	-6.6	-9.7
Casa Parroquial, Chile	ACL-0081	CAP-0022	R rib	0.70754	-6.9	-10.2
Caspana, Chile	ACL-0085	CAS-0013	URM3	0.707629 ^b	-4.9 ^c	-7.5
Caspana, Chile	ACL-0086	CAS-0015	URM1	0.707701 ^b	-3.3 ^c	-5.5
Caspana, Chile	ACL-0098	CAS-0031	URM1	0.70769	-3.3 ^c	-5.4
Caspana, Chile	ACL-0099	CAS-0032	URM2	0.70762	-4.1 ^c	-6.4
Caspana, Chile	ACL-0100	CAS-0032	URM3	0.7075	-4.7 ^c	-7.3
Caspana, Chile	ACL-0101	CAS-0033	ULM1	0.70769	-3.4 ^c	-5.5
Caspana, Chile	ACL-0102	CAS-0035	URM2	0.70759	-3.7 ^c	-6.0
Caspana, Chile	ACL-0103	CAS-0042	URP2	0.70770	-4.6 ^c	-7.1
Caspana, Chile	ACL-0104	CAS-0042	URM1	0.70767	-3.5 ^c	-5.7
Caspana, Chile	ACL-0105	CAS-0047	URM3	0.70770	-3.3 ^c	-5.5
Caspana, Chile	ACL-0107	CAS-0056	LRP1	0.70768	-3.6 ^c	-5.8
Caspana, Chile	ACL-0111	CAS-0069	URC1	0.70767	-2.9 ^c	-4.9
Caspana, Chile	ACL-0112	CAS-0069	URM2	0.70767	-3.5 ^c	-5.7
Caspana, Chile	ACL-0113	CAS-S/N(11606)	ULM2	0.70768	-4.1 ^c	-6.4
Coyo Oriental, Chile	ACL-0114	CO-3938	LRC1	0.707712 ^b	-3.5	-5.6
Coyo Oriental, Chile	F1637	CO-3978	ULM2	0.707773 ^b	-5.9	-8.8
Coyo Oriental, Chile	F1638	CO-3981	ULM1	0.707628 ^b	-4.7	-7.2
Coyo Oriental, Chile	ACL-0116	CO-3984	LLP1	0.707845 ^b	-4.2	-6.7
Coyo Oriental, Chile	F1639	CO-3996	URM2	0.707825 ^b	-7.3	-10.7
Coyo Oriental, Chile	F1641	CO-4049	URM1	0.707023 ^b	-5.0	-7.6
Coyo Oriental, Chile	F1643	CO-4090	LRM1	0.708171 ^b	-3.5	-5.7
Coyo Oriental, Chile	F1644	CO-4093	LLM1	0.707713 ^b	-3.9	-6.2
Coyo Oriental, Chile	F1645	CO-4150	URM2	0.707862 ^b	-5.1	-7.8
Coyo Oriental, Chile	F1649	CO-5377	LRP2	0.707879 ^b	-7.9	-11.4
Coyo Oriental, Chile	F1651	CO-5383	LRM1	0.707684 ^b	-4.0	-6.4
Tchecar, Chile	ACL-0234	TCH-1195	URM1	0.70764	-4.8	-7.3
Tchecar, Chile	ACL-0235	TCH-1195	URM3	0.70763	-5.1	-7.8
Tchecar, Chile	ACL-0236	TCH-1196	ULM2	0.70791	-3.9	-6.2
Tchecar, Chile	ACL-0237	TCH-1196	ULM3	0.70765	-5.4	-8.1
Tchecar, Chile	ACL-0239	TCH-1208	URM3	0.70769	-6.1	-9.1
Tchecar, Chile	ACL-0240	TCH-1213	ULC1	0.70764	-4.2	-6.6
Tchecar, Chile	ACL-0241	TCH-1213	URM2	0.70766	-4.6	-7.1
Tchecar, Chile	ACL-0243	TCH-1219	ULM2	0.70767	-5.1	-7.7
<i>Moquegua Valley</i>						
Chen Chen, Peru	F1016	M1-1600	LLM1	0.706932 ^b	-6.5 ^{cd}	-9.6
Chen Chen, Peru	F1205	M1-2947	LRM1	0.719211 ^b	-2.9 ^{cd}	-5.0
Chen Chen, Peru	F1968	M1-3472	URM1	0.707031 ^b	-6.5 ^{cd}	-9.6
Chen Chen, Peru	F1988	M1-3747	RML1	0.706844 ^b	-6.3 ^{cd}	-9.3
Chen Chen, Peru	F1019	M1-3840	LLM1	0.708843 ^b	-5.8 ^{cd}	-8.7
Chen Chen, Peru	F1020	M1-S/NB092	LRM	0.709995 ^b	-6.8 ^{cd}	-9.9

(Continues)

Table 1. (Continued)

Site, country	Laboratory number	Specimen number	Material ^a	⁸⁷ Sr/ ⁸⁶ Sr ^b	$\delta^{18}\text{O}_{\text{VPDB}}$ ^{c,d}	$\text{d}^{18}\text{O}_{\text{dw(V-SMOW)}}$
Chen Chen, Peru	F1209	M1-S/NK380	LLM1	0.707422 ^b	-7.0 ^{cd}	-10.3
<i>Lake Titicaca Basin</i>						
CK-Kirawi, Bolivia	ACL-0713	CK65-1027	URM1	0.70991	-7.7	-11.2
CK-Kirawi, Bolivia	ACL-0738	CK65-1027	LRI1	0.71132	-8.6	-12.3
CK-Kirawi, Bolivia	ACL-0714	CK65-1041	URM1	0.71225	-4.8	-7.4
CK-Kirawi, Bolivia	ACL-0715	CK65-1082	ULM1	0.71181	-5.7	-8.5
CK-Kirawi, Bolivia	ACL-0716	CK65-1086	ULM1	0.71098	-8.0	-11.5
CK-Kirawi, Bolivia	ACL-0717	CK65-1100	LRM1	0.70961	-9.2	-13.1
CK-Kirawi, Bolivia	ACL-0718	CK65-1691	LLM2	0.71017	-10.3	-14.5
CK-Pocachi Kuntu, Bolivia	ACL-0710	CK104.1-3433	ULM1	0.71086	-9.4	-13.4
CK-Pocachi Kuntu, Bolivia	ACL-0711	CK104.1-3437	LRI2	0.71107	-5.0	-7.6
CK-Pocachi Kuntu, Bolivia	ACL-0712	CK104.2-3524	LLM1	0.70872	-6.9	-10.1
Lukurmata, Bolivia	ACL-0725	LKM-0043	LUM2	0.70911	-11.4	-15.9
Lukurmata, Bolivia	ACL-0730	LKM-0364	LUM1	0.70943	-10.2	-14.4
Lukurmata, Bolivia	ACL-0731	LKM-0471	LLI1	0.70955	-9.1	-12.9
Lukurmata, Bolivia	ACL-0732	LKM-0472	LLM1	0.70919	-6.2	-9.2
Lukurmata, Bolivia	ACL-0726	LKM-10407	LUM1	0.70921	-7.8	-11.3
Lukurmata, Bolivia	ACL-0727	LKM-10415	RUM1	0.70915	-9.1	-12.9
Lukurmata, Bolivia	ACL-0728	LKM-3042	RLM1	0.70924	-8.9	-12.6
Lukurmata, Bolivia	ACL-0733	LKM-5454	LUM1	0.70999	-9.6	-13.6
Lukurmata, Bolivia	ACL-0734	LKM-5454	lum2	0.70982	-10.1	-14.2
Lukurmata, Bolivia	ACL-0735	LKM-5455	LLM1	0.70972	-8.1	-11.6
Lukurmata, Bolivia	ACL-0736	LKM-8438	RLI1	0.71201	-7.1	-10.4
Lukurmata, Bolivia	ACL-0737	LKM-9272	RLP2	0.71381	-4.7	-7.3
Tiwanaku, Bolivia	F1013	AKE-08908	LRM1	0.710907 ^b	-16.6 ^{cd}	-21.1
Tiwanaku, Bolivia	ACL-0697	AKE-30902	RLM1	0.71193	-11.0	-13.7
Tiwanaku, Bolivia	F1189	AK-04931	RUI2	0.716256 ^b	-16.5 ^{c,d}	-20.9
Tiwanaku, Bolivia	ACL-0691	AK-12149	RUM1	0.7095	-10.4	-12.9
Tiwanaku, Bolivia	ACL-0692	AK-12149	LLM2	0.70937	-13.2	-16.6
Tiwanaku, Bolivia	F1187	AK-12149	RLM1	0.709513 ^b	-17.4 ^{cd}	-22.1
Tiwanaku, Bolivia	ACL-0693	AK-1777	llm2	0.71461	-6.1	-7.2
Tiwanaku, Bolivia	ACL-0694	AK-21264	RUM1	0.71156	-9.8	-12.1
Tiwanaku, Bolivia	ACL-0695	AK-21264	RUM3	0.71019	-11.9	-14.9
Tiwanaku, Bolivia	ACL-0696	AK-21265	LUM1	0.71188	-9.5	-11.7
Tiwanaku, Bolivia	F1014	CJ-35250	URI2	0.709674 ^b	-15.8 ^{c,d}	-20.1
Tiwanaku, Bolivia	ACL-1481	MK-1065	LRM1	0.70947	-8.6	-10.5
Tiwanaku, Bolivia	ACL-1483	MK-29412-8	URM1	0.70861	-9.9	-12.2
Tiwanaku, Bolivia	ACL-1480	MK-31292	ULM1	0.70824	-10.5	-13.0
Tiwanaku, Bolivia	ACL-1485	MK-39760	URM1	0.70960	-9.6	-11.7
Tiwanaku, Bolivia	ACL-1482	MK-39786	LRM1	0.71152	-8.4	-10.2
Tiwanaku, Bolivia	ACL-1486	MK-4599	LRM1	0.70955	-5.2	-5.9
Tiwanaku, Bolivia	ACL-0684	MK-0764	RLP1	0.70957	-10.1	-12.4
Tiwanaku, Bolivia	ACL-0685	MK-0799	LLM1	0.71082	-10.3	-12.7
Tiwanaku, Bolivia	ACL-0687	MK-0874-2	LUM1	0.70879	-8.5	-10.3
Tiwanaku, Bolivia	ACL-0688	MK-0876	RLM1	0.70885	-9.0	-11.0
Tiwanaku, Bolivia	ACL-0690	MK-0985	RLM3	0.70839	-9.8	-12.0
Tiwanaku, Bolivia	ACL-0681	MK-39787	LUC	0.71056	-9.5	-11.7
Tiwanaku, Bolivia	ACL-0682	MK-39796	LLC	0.70779	-10.1	-12.4
Tiwanaku, Bolivia	F2952	PUMA-A12	LRM2	0.710812 ^b	-12.2	-15.3
Tiwanaku, Bolivia	F2953	PUMA-A12	LRM1	0.710284 ^b	-11.3	-14.1
Tiwanaku, Bolivia	F2954	PUMA-A12	LRP2	0.71113	-11.7	-14.6
Tiwanaku, Bolivia	F2959	PUMA-A12	R radius	0.709469 ^b	-8.6	-10.5
Tiwanaku, Bolivia	ACL-0698	PUT-20836	LUM2	0.71478	-8.1	-9.8
Tiwanaku, Bolivia	F1215	PUT-20995	ULM1	0.709523 ^b	-17.0 ^{c,d}	-21.5
Tiwanaku, Bolivia	F1022	PUT-24106	LRM1	0.711303 ^b	-16.7 ^{c,d}	-21.2
Tiwanaku, Bolivia	ACL-0699	PUT-25785-1	RUM1	0.71195	-8.6	-10.5
Tiwanaku, Bolivia	ACL-0701	PUT-25940-1	LLI2	0.71319	-7.7	-9.3
Tiwanaku, Bolivia	ACL-0702	PUT-25940-2	RUM1	0.71001	-7.8	-9.4
Tiwanaku, Bolivia	ACL-0703	PUT-30499	RLM1	0.71346	-8.3	-10.1
TLOBS, Bolivia	ACL-0704	TLOBS-0001	RUM1	0.71293	-9.6	-11.9

(Continues)

Table 1. (Continued)

Site, country	Laboratory number	Specimen number	Material ^a	⁸⁷ Sr/ ⁸⁶ Sr ^b	$\delta^{18}\text{O}_{\text{VPDB}}$ ^{c,d}	$\text{d}^{18}\text{O}_{\text{dw(V-SMOW)}}$
TMV-228, Bolivia	ACL-0709	TMV228-0196	RLI2	0.70748	-10.1	-12.5
TMV-Tilata, Bolivia	ACL-0705	TMV101-0345	RLM1	0.70930	-8.3	-10.1
TMV-Tilata, Bolivia	ACL-0706	TMV101-0406	RUM1	0.70934	-9.9	-12.1
TMV-Tilata, Bolivia	ACL-0707	TMV101-0406	RLI2	0.70944	-10.4	-12.8
TMV-Tilata, Bolivia	ACL-0708	TMV101-0468	LUM1	0.70827	-10.6	-13.2
<i>Nazca Drainage</i>						
Aja, Peru	ACL-0272	FMNH-170912	LLM3	0.706653 ^b	-9.1 ^c	-12.9
Cahuachi, Peru	ACL-0260	FMNH-171240	LLM1	0.706692 ^b	-8.7 ^c	-12.5
Cahuachi, Peru	ACL-0263	FMNH-171263	LRM2	0.706251 ^b	-8.7 ^c	-12.4
Cahuachi, Peru	ACL-0266	FMNH-171300	LLP1	0.706995 ^b	-7.9 ^c	-11.4
Cahuachi, Peru	ACL-0267	FMNH-171307	LLP1	0.706627 ^b	-6.6 ^c	-9.8
Cahuachi, Peru	ACL-0270	FMNH-171187	LRM2	0.706134 ^b	-8.9 ^c	-12.7
Cahuachi, Peru	ACL-0271	FMNH-171135	LRM3	0.706594 ^b	-9.2 ^c	-13.1
Cahuachi, Peru	ACL-0273	FMNH-170222	URP1	0.708669 ^b	-3.8 ^c	-6.1
Cahuachi, Peru	ACL-0276	FMNH-171096	URM3	0.706328 ^b	-9.6 ^c	-13.5
Cahuachi, Peru	ACL-0277	FMNH-170224	URM1	0.707524 ^b	-6.1 ^c	-9.1
Cahuachi, Peru	ACL-0278	FMNH-171097	ULM1	0.706493 ^b	-7.8 ^c	-11.2
Cahuachi, Peru	ACL-0280	FMNH-171098	ULP2	0.706486 ^b	-4.1 ^c	-6.4
Cahuachi, Peru	ACL-0282	FMNH-171136	ULI2	0.706593 ^b	-8.6 ^c	-12.3
Cahuachi, Peru	ACL-0283	FMNH-171186	LRM2	0.706405 ^b	-9.0 ^c	-12.9
Cahuachi, Peru	ACL-0284	FMNH-171099	URM3	0.706950 ^b	-10.6 ^c	-14.9
Cahuachi, Peru	ACL-0286	FMNH-171185	LRM2	0.707490 ^b	-8.0 ^c	-11.5
Cahuachi, Peru	ACL-0287	FMNH-171100	URM1	0.706156 ^b	-8.2 ^c	-11.8
Cantayo, Peru	ACL-0262	FMNH-170998	LRM1	0.707803 ^b	-7.9 ^c	-11.3
Cantayo, Peru	ACL-0264	FMNH-171025	LLM3	0.706856 ^b	-10.0 ^c	-14.1
Cantayo, Peru	ACL-0265	FMNH-170993	LRM2	0.706273 ^b	-7.8 ^c	-11.3
Cantayo, Peru	ACL-0269	FMNH-171023	LLM2	0.706314 ^b	-8.9 ^c	-12.7
Cantayo, Peru	ACL-0275	FMNH-171008	LLM1	0.708860 ^b	-1.8 ^c	-3.6
Cantayo, Peru	ACL-0285	FMNH-171058	LRM1	0.706586 ^b	-8.3 ^c	-11.9
Majoro Chico, Peru	ACL-0259	FMNH-170469	LLM1	0.706575 ^b	-8.3 ^c	-11.9
Majoro Chico, Peru	ACL-0261	FMNH-170493	LRM1	0.706323 ^b	-8.8 ^c	-12.5
Majoro Chico, Peru	ACL-0268	FMNH-170499	LRM3	0.707318 ^b	-7.2 ^c	-10.5
Majoro Chico, Peru	ACL-0279	FMNH-170489	URM1	0.706340 ^b	-4.8 ^c	-7.3
Majoro Chico, Peru	ACL-0281	FMNH-170463	LRM2	0.707024 ^b	-9.7 ^c	-13.8
Paredones, Peru	ACL-0274	FMNH-170157	LLM1	0.706437 ^b	-8.5 ^c	-12.2

^aMaterials include both archaeological tooth enamel and bone. Tooth enamel samples are identified according to their position in the maxilla (U) or mandible (L), location on the right (R) or left (L) and tooth type (e.g. M1 for the first molar). Deciduous teeth are identified in lower-case letters.

^bStrontium isotope data reported to the sixth decimal place and marked with a 'b' were obtained at the Geochronology and Isotope Geochemistry Laboratory at the University of North Carolina at Chapel Hill using the thermal ionisation mass spectrometer (TIMS). All other strontium isotope data were obtained in the W.M. Keck Foundation Laboratory for Environmental Biogeochemistry at Arizona State University using a multi-collector inductively-coupled plasma mass spectrometer (MC-ICP-MS).

^cThese preliminary oxygen isotope data were published elsewhere (Knudson & Price, 2007; Knudson & Torres-Rouff, in press; Knudson *et al.*, in press).

^dSamples marked with a 'd' were analysed at the Stable Isotope Laboratory in the Department of Geosciences at the University of Arizona using a Finnigan MAT 253 mass spectrometer equipped with a Kiel III automated carbonate sampling device (Knudson & Price, 2007). All other oxygen isotope data were obtained in the W.M. Keck Foundation Laboratory for Environmental Biogeochemistry at Arizona State University.

Knudson & Price, 2007; Torres-Rouff & Knudson, 2007). At the University of North Carolina at Chapel Hill, ⁸⁷Sr/⁸⁶Sr data were obtained using a VG Sector 54 thermal ionisation mass spectrometer (TIMS), where recent analyses of strontium carbonate standard SRM 987 yielded ⁸⁷Sr/⁸⁶Sr = 0.710245 ± 0.000018 (2σ). At Arizona State University, strontium isotopes were measured on a Neptune multi-collector induc-

tively coupled plasma mass spectrometer (MC-ICP-MS), where SRM-987 has exhibited ⁸⁷Sr/⁸⁶Sr = 0.710265 ± 0.000010 (2σ, n = 25).

Oxygen isotope data from Andean archaeological sites

Results of oxygen isotope analyses of archaeological human tooth enamel hydroxyapatite

carbonate samples using IRMS are shown in Table 1. In the Nazca Drainage of southern Peru, where the sites included date to the Early Intermediate Period (c. AD 1–600), enamel data range from $\delta^{18}\text{O}_{\text{c(VPDB)}} = -3.8\text{‰}$ to -10.6‰ with mean enamel $\delta^{18}\text{O}_{\text{c(VPDB)}} = -7.8\text{‰} \pm 2.0\text{‰}$ ($n = 29$, 1σ) (Knudson *et al.*, in press). In the Middle Horizon (c. AD 600–1100) Moquegua Valley of far southern Peru, enamel data range from $\delta^{18}\text{O}_{\text{c(VPDB)}} = -2.9\text{‰}$ to -7.0‰ with mean enamel $\delta^{18}\text{O}_{\text{c(VPDB)}} = -6.0\text{‰} \pm 1.4\text{‰}$ ($n = 7$, 1σ) (Knudson & Price, 2007). In the Middle to Late Horizon (c. AD 600–1500) sites in the Lake Titicaca Basin of western Bolivia, enamel and bone data range from $\delta^{18}\text{O}_{\text{c(VPDB)}} = -4.7\text{‰}$ to -17.4‰ with mean enamel $\delta^{18}\text{O}_{\text{c(VPDB)}} = -9.7\text{‰} \pm 2.9\text{‰}$ ($n = 63$, 1σ); preliminary oxygen isotope data from six of these individuals was published elsewhere (Knudson & Price, 2007). Finally, in the San Pedro de Atacama oases of northern Chile, enamel data from the Late Intermediate Period (c. AD 1100–1400) Loa River Valley site of Caspana ranges from $\delta^{18}\text{O}_{\text{c(VPDB)}} = -2.9\text{‰}$ to -4.9‰ , with mean enamel $\delta^{18}\text{O}_{\text{c(VPDB)}} = -3.8\text{‰} \pm 0.6\text{‰}$ ($n = 14$, 1σ) (Knudson & Torres-Rouff, in press). At the Middle Horizon (c. AD 500–1100) San Pedro de Atacama sites of Casa Parroquial, Coyo Oriental and Tchecar, enamel and bone data range from $\delta^{18}\text{O}_{\text{c(VPDB)}} = -2.9\text{‰}$ to -4.9‰ with mean enamel and bone $\delta^{18}\text{O}_{\text{c(VPDB)}} = -4.8\text{‰} \pm 1.3\text{‰}$ ($n = 37$, 1σ).

Interpretations of oxygen isotope data from Andean archaeological sites

With the exception of the Lake Titicaca Basin sites, the archaeological sites included in this study are exceptionally well-preserved and many of the individuals buried there are naturally mummified. Furthermore, numerous studies have demonstrated the resistance of enamel to diagenetic contamination, although bone can be more easily contaminated (Nelson *et al.*, 1986; Sillen & LeGros, 1991; Price *et al.*, 1992; Kohn *et al.*, 1999; Budd *et al.*, 2000; Sharp *et al.*, 2000; Hedges, 2002; Hoppe *et al.*, 2003; Lee-Thorp &

Sponheimer, 2003). As discussed elsewhere (Knudson & Price, 2007), biogenic strontium and oxygen isotope values have been demonstrated for a subset of the data presented here, with the exception of a small number of strontium isotope values from the Lake Titicaca Basin which may represent diagenetic strontium as well.

The oxygen isotope data from archaeological human enamel and bone hydroxyapatite carbonate from a variety of Andean archaeological sites shows substantial variability (Table 1, Figure 2). This variability is still apparent when the individuals interpreted as non-local to each site based on strontium isotope data are removed from the dataset (Knudson *et al.*, 2004, in press; Knudson, 2007, 2008; Knudson & Price, 2007; Knudson & Torres-Rouff, in press) (Figure 3). It is, of course, unrealistic to expect that the local regions for strontium and oxygen isotopes are isomorphic, since it is possible that an individual could be highly mobile within one geological zone while moving between many different environmental zones, or vice versa. However, in some Andean regions with constrained and relatively well-understood water sources, like the San Pedro de Atacama oases, it is highly likely that individuals who are consuming strontium from that constrained geological zone are also obtaining their oxygen from the same constrained environmental zone. However, even after removing the outliers from this dataset, based on strontium isotope signatures, there is still a very wide range of observed oxygen isotope signatures in these regions, with much overlap between different environmental zones (Figure 3).

Since some of these data were obtained from enamel that formed before or during the weaning process, it is possible that these enamel oxygen isotope signatures are enriched in ^{18}O since breast milk is enriched in ^{18}O (Roberts *et al.*, 1988). In individuals where it was possible to sample multiple dental and skeletal elements that formed at different times, both oxygen and carbon isotope signatures were used to determine the replacement of breast milk with imbibed water and the addition of solid foods, such as maize, to the diet during the weaning process (Figure 4) (e.g. Wright & Schwarcz, 1998, 1999). For example, for the individual assigned specimen

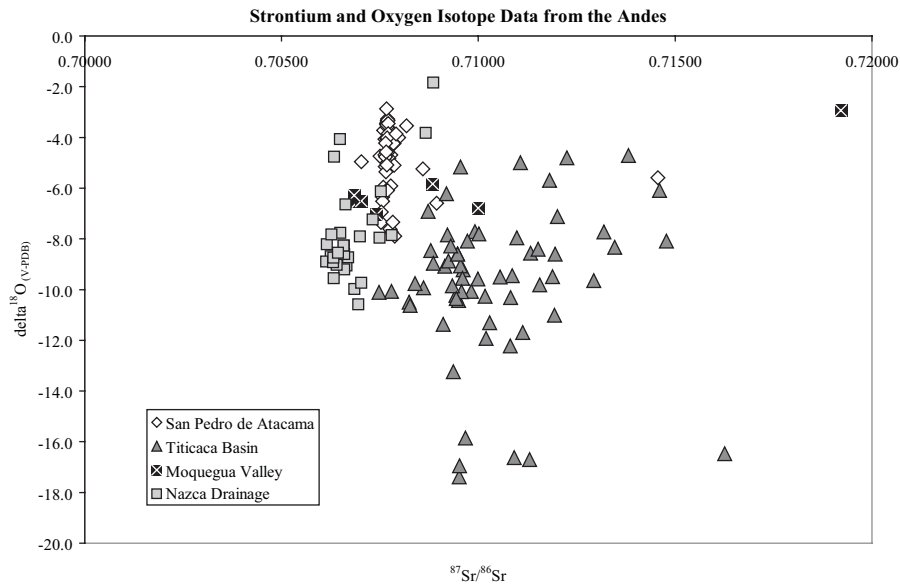


Figure 2. Oxygen and strontium isotope ratios from human tooth enamel and bone hydroxyapatite carbonate.

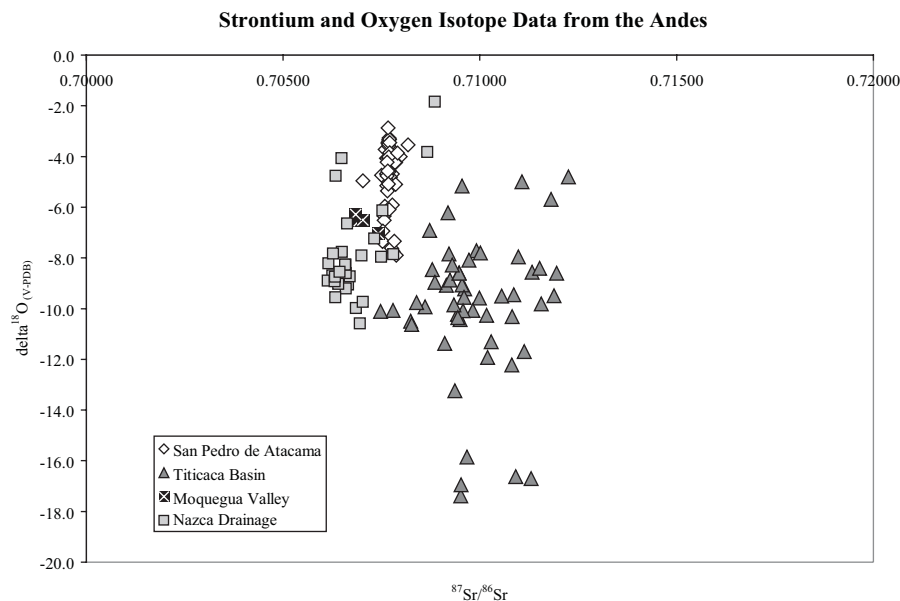


Figure 3. Oxygen and strontium isotope ratios from human tooth enamel and bone hydroxyapatite carbonate, with the individuals interpreted as non-local to each region based on strontium isotope ratios removed.

number PUMA-A12, oxygen and carbon isotope data were obtained for the following dental and skeletal elements: LRM1 ($\delta^{18}\text{O}_{\text{c(VPDB)}} = -11.3$, $\delta^{13}\text{C}_{\text{c(VPDB)}} = -12.1$), LRP2 ($\delta^{18}\text{O}_{\text{c(VPDB)}} = -11.7$, $\delta^{13}\text{C}_{\text{c(VPDB)}} = -10.5$), LRM2 ($\delta^{18}\text{O}_{\text{c(VPDB)}} = -12.2$,

$\delta^{13}\text{C}_{\text{c(VPDB)}} = -10.4$), and R radius ($\delta^{18}\text{O}_{\text{c(VPDB)}} = -8.6$, $\delta^{13}\text{C}_{\text{c(VPDB)}} = -8.8$). In the Andes, ethnographic evidence shows that the first solid foods introduced were potatoes and cereal grains such as barley, and children were breastfed until the

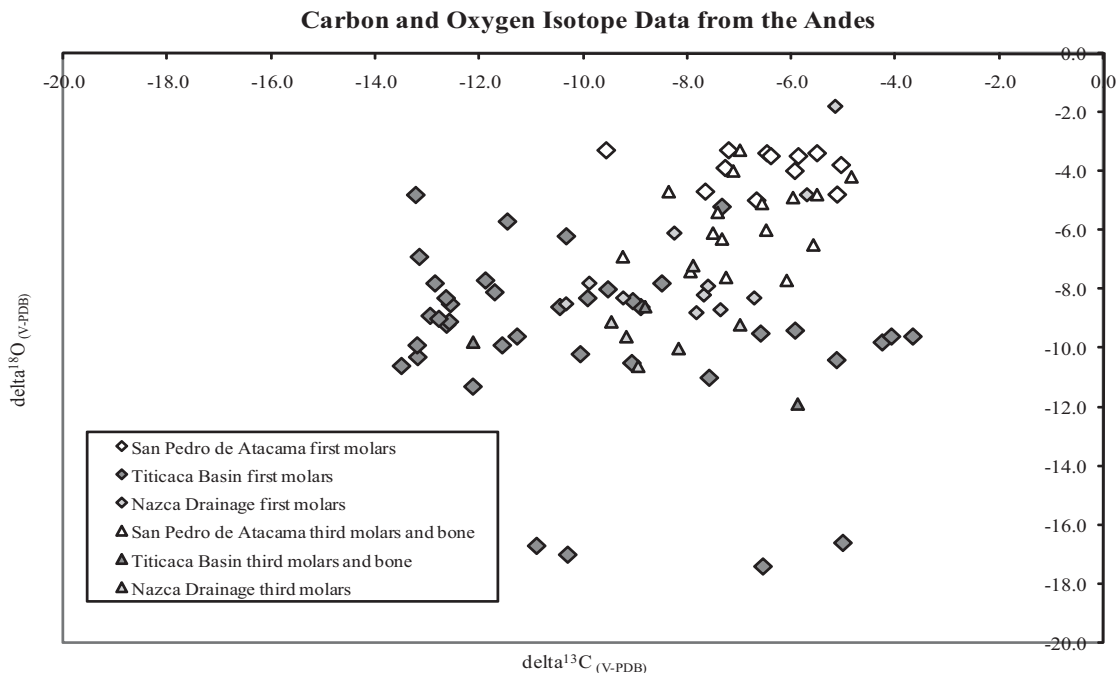


Figure 4. Oxygen and carbon isotope ratios from human tooth enamel and bone hydroxyapatite carbonate sorted by first-molar enamel that formed before and during the weaning process and third-molar enamel and bone that formed well after weaning.

age of two years (Weismantel, 1988; Leonard *et al.*, 2000). The relatively low enamel $\delta^{13}\text{C}_c$ implies that maize or other C_4 plants were not consumed in large quantities, and that it is instead likely that this individual consumed grains and tubers. Therefore, the $\delta^{13}\text{C}_c$ data imply that the changes in $\delta^{18}\text{O}_c$ in the dental elements analysed from PUMA-A12 were influenced by weaning and the addition of solid foods and water by 2–3 years of age. Similar trends are apparent in oxygen and carbon isotope data from Casa Parroquial (CAP-0001 (LRM1 ($\delta^{18}\text{O}_{c(\text{VPDB})} = -3.4$, $\delta^{13}\text{C}_{c(\text{VPDB})} = -5.5$), LLP2 ($\delta^{18}\text{O}_{c(\text{VPDB})} = -3.9$, $\delta^{13}\text{C}_{c(\text{VPDB})} = -3.9$), and Rib ($\delta^{18}\text{O}_{c(\text{VPDB})} = -6.0$, $\delta^{13}\text{C}_{c(\text{VPDB})} = -6.5$)) and CAP-0010 (ULM1 ($\delta^{18}\text{O}_{c(\text{VPDB})} = -3.8$, $\delta^{13}\text{C}_{c(\text{VPDB})} = -5.1$), URM2 ($\delta^{18}\text{O}_{c(\text{VPDB})} = -4.0$, $\delta^{13}\text{C}_{c(\text{VPDB})} = -4.6$), and LRM3 ($\delta^{18}\text{O}_{c(\text{VPDB})} = -4.8$, $\delta^{13}\text{C}_{c(\text{VPDB})} = -5.5$)). Although enamel and bone series from most of the individuals in this study were not available, a comparison of early-forming first-molar enamel carbon and oxygen isotope data with late-forming third-molar enamel and bone carbon

and oxygen isotope data shows similar trends (Figure 4). More specifically, data were analysed from first molars, which form between approximately 10 weeks before birth and three years of age (Gleiser & Hunt, 1955; Christensen & Kraus, 1965; Hillson, 1996), and third molars and bone samples, which will represent imbibed water after approximately the age of 15 years (Hillson, 1996; Olze *et al.*, 2006; Harris, 2007).

In addition to attempting to understand weaning behaviour through the introduction of solid foods, such as maize, to the diet, comparing oxygen isotope signatures in enamel that formed before and during the weaning process with enamel that formed well after the weaning process can also elucidate the role of ^{18}O -enriched breast milk in this data-set. For each region, mean enamel $\delta^{18}\text{O}_{c(\text{VPDB})}$ for first molars was compared with mean enamel $\delta^{18}\text{O}_{c(\text{VPDB})}$ from third molars and bone samples (Figure 5). In the Nazca Drainage, mean first-molar enamel $\delta^{18}\text{O}_{c(\text{VPDB})} = -7.2\% \pm 2.2\%$ ($n = 11$, 1σ) while mean third-molar enamel and bone $\delta^{18}\text{O}_{c(\text{VPDB})} = -9.3\% \pm 1.2\%$ ($n = 6$, 1σ). In

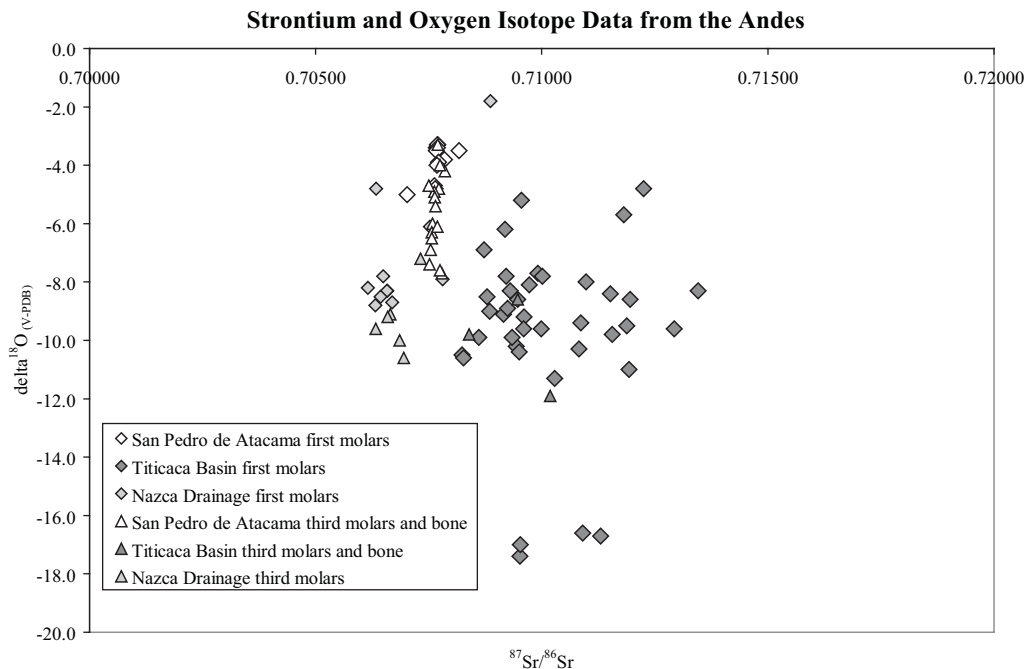


Figure 5. Oxygen and strontium isotope ratios from human tooth enamel and bone hydroxyapatite carbonate sorted by first-molar enamel that formed before and during the weaning process and third-molar enamel and bone that formed well after weaning.

the Lake Titicaca Basin, mean first-molar enamel $\delta^{18}\text{O}_{\text{c(VPDB)}} = -9.6\text{‰} \pm 2.9\text{‰}$ ($n = 39$, 1σ) while mean third-molar enamel and bone $\delta^{18}\text{O}_{\text{c(VPDB)}} = -10.1\text{‰} \pm 1.7\text{‰}$ ($n = 3$, 1σ). In San Pedro de Atacama, mean first molar enamel $\delta^{18}\text{O}_{\text{c(VPDB)}} = -3.9\text{‰} \pm 0.6\text{‰}$ ($n = 12$, 1σ), while mean third-molar enamel and bone $\delta^{18}\text{O}_{\text{c(VPDB)}} = -5.7\text{‰} \pm 1.3\text{‰}$ ($n = 16$, 1σ). In these three regions, it is clear that first molars are, as expected, enriched in ^{18}O when compared with third molars and bone (Figure 5). However, it is also clear that the variability introduced by ^{18}O enrichment in certain enamel samples does not account for all of the variability in oxygen isotope signatures that is apparent here.

Converting the observed third-molar enamel and bone $\delta^{18}\text{O}_{\text{c(VPDB)}}$ values to drinking water values ($\delta^{18}\text{O}_{\text{dw(V-SMOW)}}$) using the previously-discussed conversion equations allows a comparison of observed and expected drinking water signatures in each of the Andean regions discussed here. In the Nazca Drainage, mean third-molar enamel and bone $\delta^{18}\text{O}_{\text{dw(V-SMOW)}} = -13.2\text{‰} \pm 1.5\text{‰}$ ($n = 6$, 1σ), while in

the Lake Titicaca Basin, mean third-molar enamel and bone $\delta^{18}\text{O}_{\text{dw(V-SMOW)}} = -12.5\text{‰} \pm 2.2\text{‰}$ ($n = 3$, 1σ). Finally, in San Pedro de Atacama, mean third-molar enamel and bone $\delta^{18}\text{O}_{\text{dw(V-SMOW)}} = -8.5\text{‰} \pm 1.7\text{‰}$ ($n = 16$, 1σ). Based on these data, the mean $\delta^{18}\text{O}_{\text{dw(V-SMOW)}}$ values in the Lake Titicaca Basin and the San Pedro de Atacama region roughly correspond with the observed $\delta^{18}\text{O}_{\text{mw(V-SMOW)}}$ values discussed above. However, the situation in the coastal Nazca Drainage is much more complex, and will be discussed below.

When $\delta^{18}\text{O}_{\text{dw(V-SMOW)}}$ values from all enamel and bone samples from each region are examined, the Nazca Drainage mean $\delta^{18}\text{O}_{\text{dw(V-SMOW)}} = -11.3\text{‰} \pm 2.6\text{‰}$ ($n = 29$, 1σ). In the Moquegua Valley, mean $\delta^{18}\text{O}_{\text{dw(V-SMOW)}} = -8.9\text{‰} \pm 1.8\text{‰}$ ($n = 7$, 1σ). In the Lake Titicaca Basin, mean $\delta^{18}\text{O}_{\text{dw(V-SMOW)}} = -12.6\text{‰} \pm 3.5\text{‰}$ ($n = 63$, 1σ). Finally, in all sites in the San Pedro de Atacama region, mean $\delta^{18}\text{O}_{\text{dw(V-SMOW)}} = -7.4\text{‰} \pm 1.7\text{‰}$ ($n = 51$, 1σ). Although some of these enamel samples are undoubtedly enriched in ^{18}O , as discussed above, there are still some

regional trends in the $\delta^{18}\text{O}_{\text{dw(V-SMOW)}}$ data. For example, mean $\delta^{18}\text{O}_{\text{dw(V-SMOW)}}$ in the Lake Titicaca Basin is lower than the mean $\delta^{18}\text{O}_{\text{dw(V-SMOW)}}$ in the lower-altitude Moquegua Valley and San Pedro de Atacama region. This trend is similar to expected differences in the *puna*, *suní* and *quechua* zones, and the *yungas*, and matches observed $\delta^{18}\text{O}_{\text{mw(V-SMOW)}}$ in precipitation and groundwater in these zones. However, in the coastal Nazca Drainage, mean $\delta^{18}\text{O}_{\text{dw(V-SMOW)}}$ values are much lower than the expected values based on observed $\delta^{18}\text{O}_{\text{mw(V-SMOW)}}$ in precipitation in the *chala* and *yungas* zones. It is likely that this variability results from the incorporation of water sources from higher altitudes as well as long-term water storage on the coast, and demonstrates that attempting to match oxygen isotope signatures in precipitation to oxygen isotope signatures in human remains, without a more complex study of drinking water sources, is inadvisable.

In summary, it is most likely that the variability seen in oxygen isotope signatures from four environmentally distinct regions in the Andes reflects environmental variability and the complex effects of the movement of water between different environmental zones. As discussed above, various lines of evidence support the hypothesis that the basic Andean environmental trends have not changed over the past 2000 years (Shimada *et al.*, 1991; Baied & Wheeler, 1993; Messerli *et al.*, 1993; Bobst *et al.*, 2001; Hartley & Chong, 2002; Núñez *et al.*, 2002; Bush *et al.*, 2005; Ramirez *et al.*, 2007). Although there have been particular major drought events, for example in the Lake Titicaca Basin (Thompson *et al.*, 1979, 1985, 1998; Ortloff & Kolata, 1993; Binford *et al.*, 1997), the Lake Titicaca Basin samples included in this study do not date to the same time period as the drought at approximately AD 1100–1300. In addition, while some annual variability in precipitation patterns and river flow is expected for these regions, the bulk enamel and bone samples analysed here should provide averages of multiple years of enamel or bone formation. It is more likely that the variability in this data-set reflects the movement of water from different environmental zones, particularly from the high-altitude zones to low-altitude zones with little rainfall. Since oxygen isotope data from archae-

ological human remains has not distinguished between very different environmental zones in the South Central Andean sites analysed here, we need more research into the oxygen isotope signatures in Andean precipitation, groundwater and river water, as well as the behavioural factors that affect oxygen isotope signatures, such as the storage of drinking water and the preparation of widely-consumed beverages.

Conclusion

In conclusion, oxygen isotope data from archaeological enamel and bone hydroxyapatite carbonate demonstrate that the variability within each site, even among individuals identified as local based on strontium isotope signatures, is greater than the variability between sites located in different environmental zones. While some regional trends are apparent, it would be inappropriate to attempt to identify the environmental zone in which an individual lived based on her or his oxygen isotope signature alone. However, continuing to explore and better understand the complexities of oxygen isotope analyses in the Andes, and beyond, through detailed studies of drinking water sources and their isotopic signatures will better enable scholars to use oxygen isotope data to identify archaeological residential mobility.

Acknowledgements

I would like to thank the following individuals and institutions for laboratory access, logistical support, sample preparation and invaluable collaboration: Ariel Anbar, Arizona State University Archaeological Chemistry Laboratory, Arizona State University W.M. Keck Foundation Laboratory for Environmental Biogeochemistry, Deborah Blom, James H. Burton, David Dettman, Marta Diaz-Zorita Bonilla, Field Museum of Natural History, Kathleen Forgey, Paul Fullagar, Gwyneth Gordon, John Janusek, Anthony Michaud, Rebecca Osborn, T. Douglas Price, Proyecto Arqueológico Pumapunku-Akapana, Everett Shock, Andrew Somerville, Christina Torres-Rouff, University of North Carolina at

Chapel Hill Geochronology and Isotope Geochemistry Laboratory, University of Wisconsin at Madison Laboratory for Archaeological Chemistry, Jonathan Wiggins, Hope Williams, Ryan Williams, Sloan Williams and Jason Yaeger. Preliminary interpretations of these data were presented at the 73rd Society for American Archaeology Annual Meeting, 26–30 March 2008, in the session 'Oxygen Isotopes as Tracers of Human Mobility'. I would like to thank the session organisers, James H. Burton and T. Douglas Price, for their invitation to participate, and the session participants for their thought-provoking research. I would also like to thank the editors of this special section, Drs Ramiro Barbarena, Adolfo Gil, Gustavo Neme and Robert Tykot, for their invitation to participate, and for their helpful editorial comments. This manuscript was also strengthened by constructive comments from Christine White and two anonymous reviewers, and I thank them for their time and expertise. Finally, I would like to gratefully acknowledge the following funding sources: National Science Foundation (BCS-0202329, BCS-0514624, BCS-0721388, and BCS-0721229), Arizona State University Institute for Social Science Research Catalyst Grant, Arizona State University School of Human Evolution and Social Change, and the Field Museum of Natural History.

References

- Andrus CFT, Crowe DE, Sandweiss DH, Reitz EJ, Romanek CS. 2002. Otolith delta ¹⁸O record of mid-Holocene sea surface temperatures in Peru. *Science* **295**: 1508–1511.
- Andrus CFT, Crowe DE, Sandweiss DH, Reitz EJ, Romanek CS, Maasch KA. 2003. Response to comment on "Otolith delta ¹⁸O record of mid-Holocene sea surface temperatures in Peru". *Science* **299**: 203b.
- Andrushko VA, Buzon MR, Simonetti A, Creaser RA. 2007. Strontium isotope evidence for prehistoric migration in the valley of Cuzco, Peru: A diachronic study of pre-Inca and Inca populations. *American Journal of Physical Anthropology* **S44**: 64.
- Andrushko VA, Buzon MR, Simonetti A, Creaser RA. In press. Strontium isotope evidence for prehistoric migration at Choquepukio, valley of Cuzco, Peru. *Latin American Antiquity*.
- Aravena R, Suzuki O, Pollastri A. 1989. Coastal fog and its relation to ground water in the IV region of northern Chile. *Chemical Geology* **79**: 83–91.
- Baied CA, Wheeler JC. 1993. Evolution of high Andean puna ecosystems: environment climate, and culture change over the last 12,000 years in the central Andes. *Mountain Research and Development* **13**: 145–156.
- Balasse M, Tresset A, Ambrose SH. 2006. Stable isotope evidence ($\delta^{13}\text{C}$, $\delta^{18}\text{O}$) for winter feeding on seaweed by Neolithic sheep of Scotland. *Journal of Zoology* **270**: 170–176.
- Bearez P, DeVries TJ, Ortlieb L. 2003. Comment on "Otolith delta ¹⁸O record of mid-Holocene sea surface temperatures in Peru". *Science* **299**: 203a.
- Benson LV, Hattori EM, Taylor HE, Poulson SR, Jolie EA. 2006. Isotope sourcing of prehistoric willow and tule textiles recovered from western Great Basin rock shelters and caves – proof of concept. *Journal of Archaeological Science* **33**: 1588–1599.
- Bentley RA. 2006. Strontium isotopes from the earth to the archaeological skeleton: a review. *Journal of Archaeological Method and Theory* **13**: 135–187.
- Binford MW, Kolata AL. 1996. The natural and human setting. In *Tiwanaku and its Hinterland: Archaeology and Paleocology of an Andean Civilization, Volume 1*. Kolata AL (ed.). Smithsonian Institution Press: Washington, DC; 23–56.
- Binford MW, Kolata AL, Brenner M, Janusek JW, Seddon MT, Abbott M, Curtis JH. 1997. Climate variation and the rise and fall of an Andean civilization. *Quaternary Research* **47**: 235–248.
- Bobst AL, Lowenstein TK, Jordan TE, Godfrey LV, Ku T-L, Luo S. 2001. A 106 ka paleoclimate record from drill core of the Salar de Atacama, northern Chile. *Paleogeography, Paleoclimatology, Paleocology* **173**: 21–42.
- Bowen GJ, Wilkinson B. 2002. Spatial distribution of $\{\delta^{18}\text{O}\}$ in meteoric precipitation. *Geology* **30**: 315–318.
- Browman DL. 1981. Prehistoric nutrition and medicine in the Lake Titicaca basin. In *Health in the Andes*, Bastien JW, Donahue JM (eds.). American Anthropological Association: Washington, DC; 103–118.
- Brush SB. 1982. The natural and human environment of the central Andes. *Mountain Research and Development* **2**: 19–38.
- Bryant JD, Luz B, Froelich PN. 1994. Oxygen isotopic composition of fossil horse tooth phosphate as a record of continental paleoclimate. *Paleogeography, Paleoclimatology, Paleocology* **107**: 303–316.
- Budd P, Montgomery J, Barreiro B, Thomas RG. 2000. Differential diagenesis of strontium in archaeologi-

- cal human dental tissues. *Applied Geochemistry* **15**: 687–694.
- Bush MB, Hansen BCS, Rodbell DT, Seltzer GO, Young KR, León B, Abbott MB, Silman MR, Gosling WD. 2005. A 17,000-year history of Andean climate and vegetation change from Laguna de Chochos, Peru. *Journal of Quaternary Science* **20**: 703–714.
- Buzon MR, Conlee CA, Simonetti A, Creaser RA. 2008. An Investigation of Human Migration and Burial Practices in the Nasca Region Using Strontium Isotope Analysis. Paper presented at the 2008 Society for American Archaeology Meetings, March 26–30, Vancouver, British Columbia.
- Carré M, Bentaleb I, Fontugne M, Lavallée D. 2005. Strong El Niño events during the early Holocene: stable isotope evidence from Peruvian sea shells. *The Holocene* **15**: 42–47.
- Carré M, Bentaleb I, Blamart D, Ogle N, Cardenas F, Zevallos S, Kalin RM, Ortlieb L, Fontugne M. 2006. Stable isotopes and sclerochronology of the bivalve *Mesodesma donacium*: potential application to Peruvian paleoceanographic reconstructions. *Applied Geochemistry* **22**: 4–25.
- Caviedes CN. 1975. El Niño 1972: its climatic, ecological, human, and economic implications. *Geographical Review* **65**: 493–509.
- Caviedes CN. 1984. El Niño. 1982–83. *Geographical Review* **74**: 267–290.
- Christensen GJ, Kraus BS. 1965. Initial calcification of the human permanent first molar. *Journal of Dental Research* **44**: 1338–1342.
- Coplen TB. 1994. Reporting of stable hydrogen, carbon, and oxygen isotope abundances. *Pure and Applied Chemistry* **66**: 271–276.
- Coplen TB, Kendall C, Hoppie J. 1983. Comparison of stable isotope reference samples. *Nature* **302**: 236–238.
- Craig H. 1961a. Isotopic variations in meteoric waters. *Science* **133**: 1702–1703.
- Craig H. 1961b. Standard for reporting concentrations of deuterium and oxygen-18 in natural waters. *Science* **133**: 1833–1834.
- Dansgaard W. 1964. Stable isotopes in precipitation. *Tellus* **16**: 436–468.
- Dillehay TD, Kolata AL. 2004. Long-term human response to uncertain environmental conditions in the Andes. *Proceedings of the National Academy of Sciences* **101**: 4325–4330.
- Dufour E, Holmden C, Neer WV, Zazzo A, Patterson WP, Degryse P, Keppens E. 2007. Oxygen and strontium isotopes as provenance indicators of fish at archaeological sites: The case study of Sagalassos, SW/Turkey. *Journal of Archaeological Science* **34**: 1226–1239.
- Dupras TL, Schwarcz HP, Fairgrieve SI. 2001. Infant feeding and weaning practices in Roman Egypt. *American Journal of Physical Anthropology* **115**: 204–212.
- Dupras TL, Tocheri MW. 2007. Reconstructing infant weaning histories at Roman period Kellis, Egypt using stable isotope analysis of dentition. *American Journal of Physical Anthropology* **134**: 63–74.
- Ehleringer JR, Bowen GJ, Chesson LA, West AG, Podlesak DW, Cerling TE. 2008. Hydrogen and oxygen isotope ratios in human hair are related to geography. *Proceedings of the National Academy of Sciences* **105**: 2788–2793.
- Epstein S, Mayeda T. 1953. Variation of O¹⁸ content of waters from natural sources. *Geochimica et Cosmochimica Acta* **4**: 213–224.
- Fuller BT, Richards MP, Mays S. 2003. Stable carbon and nitrogen isotope variations in tooth dentine serial sections from Wharram Percy. *Journal of Archaeological Science* **30**: 1673–1684.
- Fuller BT, Molleson TI, Harris DA, Hedges REM. 2006. Isotopic evidence for breastfeeding and possible adult dietary differences from late/sub-Roman Britain. *American Journal of Physical Anthropology* **129**: 45–54.
- Gat JR. 1996. Oxygen and hydrogen isotopes in the hydrologic cycle. *Annual Review of Earth and Planetary Sciences* **24**: 225–262.
- Gleiser I, Hunt EE Jr. 1955. The permanent mandibular first molar: its calcification, eruption, and decay. *American Journal of Physical Anthropology* **13**: 253–281.
- Grootes PM, Stuiver M. 1989. Oxygen isotope changes in tropical ice, Quelccaya, Peru. *Journal of Geophysical Research* **94**: 1187–1194.
- Harris EF. 2007. Mineralization of the mandibular third molar: a study of American blacks and whites. *American Journal of Physical Anthropology* **132**: 98–109.
- Hartley AJ, Chong G. 2002. Late Pliocene age for the Atacama Desert: implications for the desertification of western South America. *Geology* **30**: 43–46.
- Hedges RE. 2002. Bone diagenesis: an overview of progress. *Archaeometry* **44**: 319–328.
- Herring DA, Saunders SR, Katzenberg MA. 1998. Investigating the weaning process in past populations. *American Journal of Physical Anthropology* **105**: 425–439.
- Hillson S. 1996. *Dental Anthropology*. Cambridge University Press: Cambridge.
- Hoppe KA, Koch PL, Furutani TT. 2003. Assessing the preservation of biogenic strontium in fossil bones and tooth enamel. *International Journal of Osteoarchaeology* **13**: 20–28.
- Houston J. 2006. Variability of precipitation in the Atacama Desert: its causes and hydrological impact. *International Journal of Climatology* **26**: 2181–2198.

- Houston J, Hartley AJ. 2003. The central Andean west-slope rainshadow and its potential contribution to the origin of hyper-aridity in the Atacama Desert. *International Journal of Climatology* **23**: 1453–1464.
- Iacumin P, Bocherens H, Mariotti A, Longinelli A. 1996a. Oxygen isotope analyses of co-existing carbonate and phosphate in biogenic apatite: a way to monitor diagenetic alteration of bone phosphate? *Earth and Planetary Science Letters* **142**: 1–6.
- Iacumin P, Cominotto D, Longinelli A. 1996b. A stable isotope study of mammal skeletal remains of mid-Pleistocene age, Arago Cave, Eastern Pyrenees, France. Evidence of taphonomic and diagenetic effects. *Paleogeography, Paleoclimatology, Paleocology* **126**: 151–160.
- IAEA/WMO. 2006. *Global network of isotopes in precipitation. The GNIP database*. Available at: <http://isohis.iaea.org>.
- Ingraham NL, Matthews RA. 1995. The importance of fog-drip water to vegetation: Point Reyes Peninsula, California. *Journal of Hydrology* **164**: 269–285.
- Kelly S, Heaton K, Hoogewerff J. 2005. Tracing the geographical origin of food: The application of multi-element and multi-isotope analysis. *Trends in Food Science and Technology* **16**: 555–567.
- Killingley JS. 1980. Migrations of California gray whales tracked by oxygen-18 variations in their epizoic barnacles. *Science* **207**: 759–760.
- Killingley JS, Lutcavage M. 1983. Loggerhead turtle movement reconstructed from ^{18}O and ^{13}C profiles from commensal barnacle shells. *Estuarine Coastal Shelf Science* **16**: 345–349.
- Knudson KJ. 2004. *Tiwanaku residential mobility in the South Central Andes: identifying archaeological human migration through strontium isotope analysis*. PhD dissertation, University of Wisconsin at Madison.
- Knudson KJ. 2007. La influencia de Tiwanaku en San Pedro de Atacama: Una investigación por los isótopos del estroncio. *Estudios Atacamenos* **33**: 7–24.
- Knudson KJ. 2008. Tiwanaku influence in the south central Andes: Strontium isotope analysis and Middle Horizon migration. *Latin American Antiquity* **19**: 3–23.
- Knudson KJ, Price TD, Buikstra JE, Blom DE. 2004. The use of strontium isotope analysis to investigate Tiwanaku migration and mortuary ritual in Bolivia and Peru. *Archaeometry* **46**: 5–18.
- Knudson KJ, Tung T, Nystrom KC, Price TD, Fullagar PD. 2005. The origin of the Juch'uypampa Cave mummies: strontium isotope analysis of archaeological human remains from Bolivia. *Journal of Archaeological Science* **32**: 903–913.
- Knudson KJ, Williams SR, Osborne R, Forgey K, Williams PR. In press. The geographic origins of Nasca trophy heads in the Kroeber collection using strontium, oxygen, and carbon isotope data. *Journal of Anthropological Archaeology*.
- Knudson KJ, Buikstra JE. 2007. Residential mobility and resource use in the Chiribaya polity of southern Peru: strontium isotope analysis of archaeological tooth enamel and bone. *International Journal of Osteoarchaeology* **17**: 563–580.
- Knudson KJ, Price TD. 2007. Utility of multiple chemical techniques in archaeological residential mobility studies: case studies from Tiwanaku- and Chiribaya-affiliated sites in the Andes. *American Journal of Physical Anthropology* **132**: 25–39.
- Knudson KJ, Tung TA. 2007. Using archaeological chemistry to investigate the geographic origins of trophy heads in the central Andes: strontium isotope analysis at the Wari site of Conchopata. In *Archaeological Chemistry: Analytical Techniques and Archaeological Interpretation*, Glascock MD, Speakman RJ, Popelka-Filcoff RS (eds). American Chemical Society: Washington, DC, 99–113.
- Knudson KJ, Blom DE. In press. The complex relationship between Tiwanaku mortuary identity and geographic origin in the south central Andes. In *Bioarchaeology and Identity in the Americas*, Knudson KJ, Stojanowski CM (eds). University Press of Florida: Gainesville, FL.
- Knudson KJ, Torres-Rouff C. In press. Investigating cultural heterogeneity in San Pedro de Atacama, northern Chile through biogeochemistry and bioarchaeology. *American Journal of Physical Anthropology*.
- Koch PL. 1998. Isotopic reconstruction of past continental environments. *Annual Review of Earth and Planetary Sciences* **26**: 573–613.
- Koch PL, Tuross N, Fogel M. 1997. The effects of sample treatment and diagenesis on the isotopic integrity of carbonate in biogenic hydroxylapatite. *Journal of Archaeological Science* **24**: 417–429.
- Kohn MJ, Schoeninger MJ, Barker WW. 1999. Altered states: effects of diagenesis on fossil tooth chemistry. *Geochimica et Cosmochimica Acta* **63**: 2737–2747.
- Lee-Thorp J. 2002. Two decades of progress towards understanding fossilization processes and isotopic signals in calcified tissue minerals. *Archaeometry* **44**: 435–446.
- Lee-Thorp JA, Merwe NJvd. 1991. Aspects of the chemistry of modern and fossil biological apatites. *Journal of Archaeological Science* **18**: 343–354.
- Lee-Thorp J, Sponheimer M. 2003. Three case studies used to reassess the reliability of fossil bone and enamel isotope signals for paleodietary studies. *Journal of Anthropological Archaeology* **22**: 208–216.

- Leonard WR, Dewalt KM, Stansbury JP, McCoston MK. 2000. Influence of dietary quality on the growth of highland and coastal Ecuadorian children. *American Journal of Human Biology* **12**: 825–837.
- Longinelli A. 1984. Oxygen isotopes in mammal bone phosphate: a new tool for paleohydrological and paleoclimatological research? *Geochimica et Cosmochimica Acta* **48**: 385–390.
- Luz B, Kolodny Y, Horowitz M. 1984. Fractionation of oxygen isotopes between mammalian bone-phosphate and environmental drinking water. *Geochimica et Cosmochimica Acta* **48**: 1689–1693.
- Luz B, Kolodny Y. 1985. Oxygen isotope variations in phosphate of biogenic apatites, IV. Mammal teeth and bone. *Earth and Planetary Science Letters* **75**: 29–36.
- Magaritz M, Aravena R, Pena H, Suzuki O, Grilli A. 1990. Source of ground water in the deserts of northern Chile: Evidence of deep circulation of ground water from the Andes. *Ground Water* **28**: 513–517.
- Magiligan FJ, Goldstein PS. 2001. El Niño floods and culture change: a late Holocene flood history for the Río Moquegua, southern Peru. *Geology* **29**: 431–434.
- Masuda S. 1985. Algae collectors and lomas. In *Andean Ecology and Civilization*, Masuda S, Shimada I, Morris C (eds). University of Tokyo: Tokyo, 233–250.
- Mays S. 2003. Bone strontium: calcium ratios and duration of breastfeeding in a Mediaeval skeletal population. *Journal of Archaeological Science* **30**: 731–741.
- Messerli B, Grosjean M, Bonani G, Bürgi A, Geyh MA, Graf K, Ramseyer K, Romero H, Schotterer U, Schreier H, Vuille M. 1993. Climate change and natural resource dynamics of the Atacama altiplano during the last 18,000 years: a preliminary synthesis. *Mountain Research and Development* **13**: 117–127.
- Moore JD. 1991. Cultural responses to environmental catastrophes: post-El Niño subsistence on the prehistoric north coast of Peru. *Latin American Antiquity* **2**: 27–47.
- Munro LE, Longstaffe FJ, White CD. 2007. Burning and boiling of modern deer bone: effects on crystallinity and oxygen isotope composition of bioapatite phosphate. *Geochimica et Cosmochimica Acta* **249**: 90–102.
- Nelson BK, DeNiro MJ, Schoeninger MJ, DePaolo DJ, Hare PE. 1986. Effects of diagenesis on strontium, carbon, nitrogen, and oxygen concentration and isotopic concentration of bone. *Geochimica et Cosmochimica Acta* **50**: 1941–1949.
- Núñez L, Grosjean M, Cartajena I. 2002. Human occupations and climate change in the Puna de Atacama, Chile. *Science* **298**: 821–824.
- O'Brien DM, Wooller MJ. 2007. Tracking human migration using stable oxygen and hydrogen isotope analyses of hair and urine. *Rapid Communications in Mass Spectrometry* **21**: 2422–2430.
- Olze A, van Niekerk P, Schmidt S, Wernecke K-D, Rosing FW, Geserick G, Schumeling A. 2006. Studies on the progress of third-molar mineralisation in a black African population. *HOMO - Journal of Comparative Human Biology* **57**: 209–217.
- Orlove BS, Chiang JCH, Cane MA. 2000. Forecasting Andean rainfall and crop yield from the influence of El Niño on Pleiades visibility. *Nature* **403**: 68–71.
- Ortloff CR, Kolata AL. 1993. Climate and collapse: agroecological perspectives on the decline of the Tiwanaku state. *Journal of Archaeological Science* **20**: 195–221.
- Price TD, Blitz J, Burton JH, Ezzo J. 1992. Diagenesis in prehistoric human bone: problems and solutions. *Journal of Archaeological Science* **19**: 513–529.
- Prowse TL, Schwarcz HP, Garnsey P, Knyf M, Macchiarelli R, Bondioli L. 2007. Isotopic evidence for age-related immigration to imperial Rome. *American Journal of Physical Anthropology* **132**: 510–519.
- Pulgar Vidal J. 1981. *Geografía del Perú: Las ocho regiones naturales del Perú*. Editorial Universo S.A.: Lima, Peru.
- Ramirez E, Hoffman G, Taupin JD, Francoua B, Ribstein P, Caillon N, Ferron FA, Landais A, Petit JR, Pouyaud B, Schotterer U, Simoes JC, Stievenard M. 2007. A new Andean deep ice core from Nevado Illimani (6350 m), Bolivia. *Earth and Planetary Science Letters* **212**: 337–350.
- Reinhard E, Torres Td, O'Neil J. 1996. $^{18}\text{O}/^{16}\text{O}$ ratios of cave bear tooth enamel: A record of climate variability during the Pleistocene. *Paleogeography, Paleoclimatology, Paleoecology* **126**: 45–49.
- Reycraft RM. 2000. Long-term human response to El Niño in south coastal Peru. In *Environmental Disaster and the Archaeology of Human Response*, Bawden G, Reycraft RM (eds). Maxwell Museum of Anthropology: Albuquerque, NM; 99–120.
- Richards MP, Mays S, Fuller BT. 2002. Stable carbon and nitrogen isotope values of bone and teeth reflect weaning age at the medieval Wharram Percy site, Yorkshire, UK. *American Journal of Physical Anthropology* **119**: 205–210.
- Roberts SB, Coward WA, Ewing G, Savage J, Cole TJ, Lucas A. 1988. Effect of weaning on accuracy of doubly labeled water method in infants. *American Journal of Physiology: Regulatory, Integrative and Comparative Physiology* **254**: R622–627.
- Roche MA, Bourges J, Cortes J, Matos R. 1991. Climatología e hidrología de la cuenca del lago Titicaca. In *El Lago Titicaca: Síntesis del conocimiento limnológico actual*, Dejoux C, Iltis A (eds). ORSTOM: La Paz. 83–104.
- Rollins HB, Richardson JB III, Sandweiss DH. 1986. The birth of El Niño: geoarchaeological implications. *Geoarchaeology: An International Journal* **1**: 3–15.

- Sandweiss DH, Richardson JB III, Reitz EJ, Rollins HB, Maasch KA. 1996. Geoarchaeological evidence from Peru for a 5000 years B.P. onset of El Niño. *Science* **273**: 1531–1533.
- Sandweiss DH, Maasch KA, Burger RL, Richardson JB III, Rollins HB, Clement A. 2001. Variation in Holocene El Niño frequencies: climate records and cultural consequences in ancient Peru. *Geology* **29**: 603–606.
- Satterlee DR. 1993. *Impact of a fourteenth century El Niño flood on an indigenous population near Ilo, Peru*. PhD dissertation, University of Florida.
- Scholl MA, Gingerick SB, Tribble GW. 2002. The influence of microclimates and fog on stable isotope signatures used in interpretation of regional hydrology: East Maui, Hawaii. *Journal of Hydrology* **264**: 170–184.
- Schurr MR. 1998. Using stable nitrogen-isotopes to study weaning behavior in past populations. *World Archaeology* **30**: 327–342.
- Shahack-Gross R, Tchernov E, Luz B. 2003. Oxygen isotopic composition of mammalian skeletal phosphate from the Natufian period, Hayonim Cave, Israel: diagenesis and paleoclimate. *Geoarchaeology* **14**: 1–13.
- Sharp ZD, Atudorei V, Furrer H. 2000. The effect of diagenesis on oxygen isotope ratios of biogenic phosphates. *American Journal of Science* **300**: 222–237.
- Shimada I, Schaaf CB, Thompson LG, Mosley-Thompson E. 1991. Cultural impacts of severe droughts in the prehistoric Andes: application of a 1,500-year ice core precipitation record. *World Archaeology* **22**: 247–270.
- Sillen A. 1989. Diagenesis of the inorganic phase of cortical bone. In *The Chemistry of Prehistoric Human Bone*, Price TD (ed.). Cambridge University Press: Cambridge, 211–228.
- Sillen A, LeGros R. 1991. Solubility profiles of synthetic apatites and of modern and fossil bone. *Journal of Archaeological Science* **16**: 661–672.
- Sillen A, Sealy JC. 1995. Diagenesis of strontium in fossil bone: a reconsideration of Nelson. *et al.* 1986. *Journal of Archaeological Science* **22**: 313–320.
- Slovak NM. 2007. *Examining imperial influence on Peru's central coast: Isotopic and cultural analyses of Middle Horizon burials at Ancon*. PhD dissertation, Stanford University, Palo Alto, CA.
- Squeo FA, Aravena R, Aguirre E, Pollastri A, Jorquera CB, Ehleringer JR. 2006. Groundwater dynamics in a coastal aquifer in north-central Chile: implications for groundwater recharge in an arid ecosystem. *Journal of Arid Environments* **67**: 240–254.
- Stichler W, Schotterer U. 2000. From accumulation to discharge: modification of stable isotopes during glacial and post-glacial processes. *Hydrological Processes* **14**: 1423–1438.
- Stuart-Williams HLQ, Schwarcz HP. 1997. Oxygen isotopic determination of climatic variation using phosphate from beaver bone, tooth enamel, and dentine. *Geochimica et Cosmochimica Acta* **61**: 2539–2550.
- Tapley TD Jr, Waylen PR. 1990. Spatial variability of annual precipitation and ENSO events in western Peru. *Hydrological Sciences* **35**: 429–446.
- Thompson LG, Hastenrath S, Arnao BM. 1979. Climatic ice core records from the tropical Quelccaya ice cap. *Science* **203**: 1240–1243.
- Thompson LG, Mosley-Thompson E, Arnao BM. 1984. El Niño-Southern Oscillation events recorded in the stratigraphy of the tropical Quelccaya ice cap, Peru. *Science* **226**: 50–53.
- Thompson LG, Mosley-Thompson E, Bolzan JF, Koci BR. 1985. A 1500-year record of tropical precipitation in ice cores from the Quelccaya ice cap, Peru. *Science* **229**: 971–973.
- Thompson LG, Davis ME, Mosley-Thompson E, Sowers TA, Henderson KA, Zagorodnov VS, Lin PN, Mikhalenko VN, Campen RK, Bolzan JF, Cole-Dai J, Francou B. 1998. A 25,000-year tropical climate history from Bolivian ice cores. *Science* **282**: 1858–1864.
- Tomczak P. 2001. *Prehistoric socio-economic relations and population organization in the lower Osmore valley of southern Peru*. PhD dissertation, University of New Mexico, Albuquerque.
- Torres-Rouff C, Knudson KJ. 2007. Examining the life history of an individual from Solcor 3, San Pedro de Atacama: combining bioarchaeology and archaeological chemistry. *Chungara* **39**: 235–257.
- Tung TA, Knudson KJ. 2006. Identifying the origin of Wari trophy heads in the ancient Andes using bioarchaeology and archaeological chemistry. *American Journal of Physical Anthropology* **129**: 178.
- Tung TA, Knudson KJ. 2008. Social identities and geographical origins of Wari trophy heads from Conchopata, Peru. *Current Anthropology* **49**(5): 915–925.
- Turner B, Kingston JD, Burger R, Salazar LC. 2006. Isotopic reconstruction of paleodiet and immigration at Machu Picchu, Peru: early results. *American Journal of Physical Anthropology* **129**: 178–179.
- Turner BL, Edwards JL, Quinn EA, Kingston JD, Gerven DPV. 2007. Age-related variation in isotopic indicators of diet at Medieval Kulubnarti, Sudanese Nubia. *International Journal of Osteoarchaeology* **17**: 1–25.
- Turner BL, Kamenov GD, Kingston JD, Armelagos GJ. 2008. Insights into immigration and social class at Machu Picchu, Peru based on oxygen, strontium, and lead isotopic analysis. *Journal of Archaeological Science* **36**: 317–322.

- Van Buren M. 2001. The archaeology of El Niño events and other 'natural' disasters. *Journal of Archaeological Method and Theory* 8: 129–150.
- Vuille M, Ammann C. 1997. Regional snowfall patterns in the high, arid Andes. *Climate Change* 36: 413–423.
- Waylen PR, Caviedes CN. 1986. El Niño and annual floods on the north Peruvian littoral. *Journal of Hydrology* 89: 141–156.
- Weismantel MJ. 1988. *Food, Gender, and Poverty in the Ecuadorian Andes*. University of Pennsylvania Press: Philadelphia.
- White CD, Spence MW, Stuart-Williams HLQ, Schwarcz HP. 1998. Oxygen isotopes and the identification of geographical origins: the Valley of Oaxaca versus the Valley of Mexico. *Journal of Archaeological Science* 25: 643–655.
- White CD, Spence MW, Longstaffe FJ, Law KR. 2000. Testing the nature of Teotihuacan imperialism at Kaminaljuyú using phosphate oxygen-isotope ratios. *Journal of Anthropological Research* 56: 535–558.
- White CD, Longstaffe FJ, Law KR. 2001. Revisiting the Teotihuacan connection at Altun Ha: oxygen-isotope analysis of tomb F-8/1. *Ancient Mesoamerica* 12: 65–72.
- White CD, Spence MW, Longstaffe FJ, Stuart-Williams H, Law KR. 2002. Geographic identities of the sacrificial victims from the Feathered Serpent Pyramid, Teotihuacan: implications for the nature of state power. *Latin American Antiquity* 13: 217–236.
- White CD, Longstaffe FJ, Law KR. 2004a. Exploring the effects of environment, physiology and diet on oxygen isotope ratios in ancient Nubian bones and teeth. *Journal of Archaeological Science* 31: 233–250.
- White CD, Spence MW, Longstaffe FJ, Law KR. 2004b. Demography and ethnic continuity in the Tlailotlacan enclave of Teotihuacan: the evidence from stable oxygen isotopes. *Journal of Anthropological Archaeology* 123: 385–403.
- White CD, Storey R, Longstaffe FJ, Spence MW. 2004c. Immigration, assimilation, and status in the ancient city of Teotihuacan: stable isotope evidence from Tlajinga 33. *Latin American Antiquity* 15: 176–197.
- White CD, Price TD, Longstaffe FJ. 2007. Residential histories of the human sacrifices at the Moon Pyramid, Teotihuacan. *Ancient Mesoamerica* 18: 159–172.
- Williams DC, Coltrain JB, Lott M, English NB, Ehleringer JR. 2005a. Oxygen isotopes in cellulose identify source water for archaeological maize in the American southwest. *Journal of Archaeological Science* 32: 931.
- Williams JS, White CD, Longstaffe FJ. 2005b. Trophic level and macronutrient shift effects associated with the weaning process in the postclassic Maya. *American Journal of Physical Anthropology* 128: 781–790.
- Wilson AS, Taylor T, Ceruti MC, Chavez JA, Reinhard J, Grimes V, Meier-Augenstein W, Cartmell L, Stern B, Richards MP, Worobey M, Barnes I, Gilbert MTP. 2007. Stable isotope and DNA evidence for ritual sequences in Inca child sacrifice. *Proceedings of the National Academy of Sciences* 104: 16456–16461.
- Wright LE, Schwarcz HP. 1998. Stable carbon and oxygen isotopes in human tooth enamel: identifying breastfeeding and weaning in prehistory. *American Journal of Physical Anthropology* 106: 1–18.
- Wright LE, Schwarcz HP. 1999. Correspondence between stable carbon, oxygen and nitrogen isotopes in human tooth enamel and dentine: infant diets at Kaminaljuyú. *Journal of Archaeological Science* 26: 1159–1170.
- Zaro G, Umire Alvarez A. 2005. Late Chiribaya agriculture and risk management along the arid Andean coast of southern Perú, AD. 1200–1400. *Geoarchaeology* 20: 717–737.
- Zazzo A, Lecuyer C, Sheppard SMF, Grandjean P, Mariotti A. 2004. Diagenesis and the reconstruction of paleoenvironments: a method to restore original $[\delta]^{18}\text{O}$ values of carbonate and phosphate from fossil tooth enamel. *Geochimica et Cosmochimica Acta* 68: 2245–2258.
- Zazzo A, Smith GR, Patterson WP, Dufour E. 2006. Life history reconstruction of modern and fossil sockeye salmon (*Oncorhynchus nerka*) by oxygen isotopic analysis of otoliths, vertebrae, and teeth: implication for paleoenvironmental reconstructions. *Earth and Planetary Science Letters* 249: 200–215.